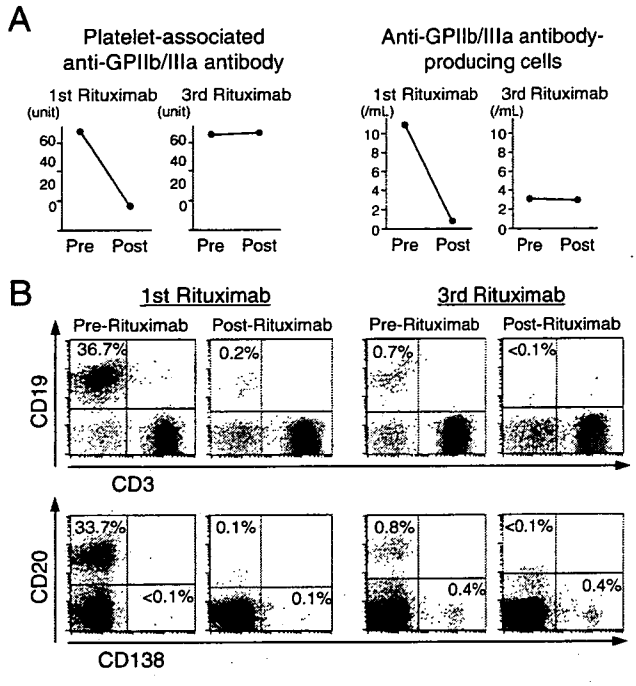

Figure 1. Serial measurements of anti-GPIIb/IIIa antibody responses and circulating B cell subsets before and after the first and third courses of rituximab. A: Platelet-associated IgG anti-GPIIb/IIIa antibody was measured by enzyme-linked immunosorbent assay using purified human GPIIb/IIIa as the antigen, and the antibody units were calculated based on a standard curve obtained from serial concentrations of a standard plasma. IgG anti-GPIIb/IIIa antibody-producing cells were detected using enzyme-linked immunospot assay and are shown in the absolute number per 1 mL of peripheral blood. B: Serial flow cytometric analysis of $CD19^+CD3^-$ B cells, $CD20^+CD138^-$ B cells, and $CD20^-CD138^+$ plasma cells. Relative proportions of the subsets of interest are shown in each panel.

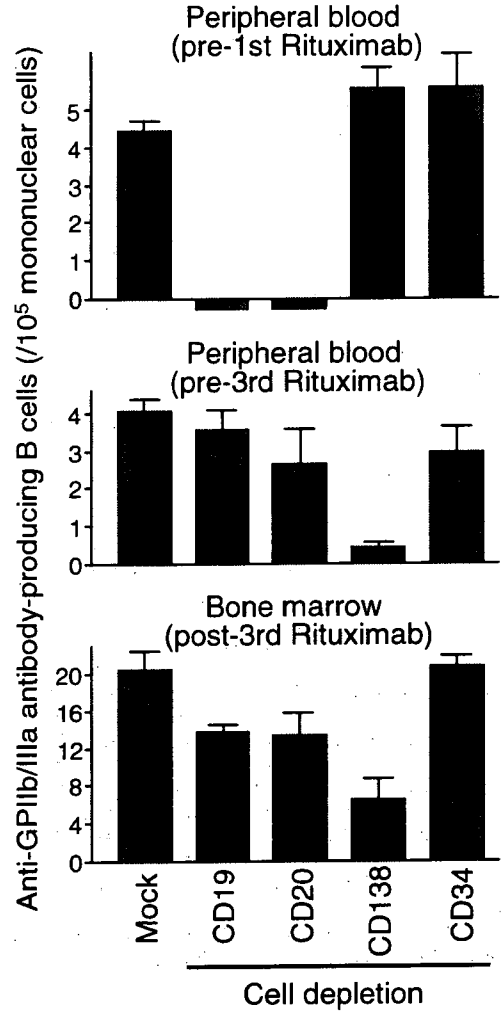

Figure 2. IgG anti-GPIIb/IIIa antibody-producing cells in mononuclear cells that were mock-treated or were depleted of $CD19^+$, $CD20^+$, $CD138^+$, or $CD34^+$ cells. IgG anti-GPIIb/IIIa antibody-producing cells in peripheral blood or bone marrow mononuclear cells were detected using enzyme-linked immunospot assay. The cell depletion was performed using magnetic bead-coupled corresponding monoclonal antibodies, followed by separation on a MACS column. The frequency of circulating anti-GPIIb/IIIa antibody-producing B cells was calculated as the number per 10^5 mononuclear cells. Results shown are the mean and standard deviation obtained from three independent wells.

the bone marrow while she was refractory to rituximab. Since rituximab, which was designed to target B lineage cells, does not eliminate plasma cells, the appearance of plasma cells producing anti-platelet autoantibodies could be one of the mechanisms of rituximab resistance. In this regard, there is increasing evidence that plasma cells can survive as long as memory B cells, and such long-lived plasma cells are thought to be involved in the pathogenesis of various autoimmune diseases through their continuous production of pathogenic autoantibodies [9]. Because anti-GPIIb/IIIa antibody-producing plasma cells were undetectable in our patient before rituximab treatment and in 10 additional ITP patients who never received rituximab, it is possible that repeated doses of rituximab might induce a compensatory shift in the dominance of autoantibody-producing cells from B cells to plasma cells, following the rituximab-induced loss of the B cells. The mechanism involved in this process remains unclear, but it might be mediated through longevity of autoantibody-producing plasma cells, because rituximab blocks differentiation of memory B cells into plasma cells. Currently, there is little information regarding the efficacy of rituximab retreatment in ITP patients who relapse after one cycle of treatment, but we should take this potential mechanism for rituximab resistance into account in developing future therapeutic strategies for refractory ITP.

Materials and Methods

Case report

A 75-year-old woman presented with multiple ecchymoses and nasal bleeding in June 2003. Physical examination revealed petechiae on her palate and scattered diffusely on her arms, legs, and trunk. Her complete blood count showed hemoglobin 8.5 g/dL, leukocyte 4.0 $\times$ $10^9 \cdot L^{-1}$ with normal differential, and platelet 12 $\times$ 10^9 L^{-1}. Coagulation and blood chemistry studies were normal. Antinuclear antibody was negative, but IgG anti-cardiolipin antibody was strongly positive (74 GPL). A bone marrow evaluation showed normocellular marrow without dysplasia or megakaryocytic hypoplasia. The patient was initially treated with prednisolone (1 mg/kg), but there was no clear platelet response, and she required frequent platelet transfusions, because of severe persistent thrombocytopenia (platelets $< 5 \times 10^9$ L^{-1}) with oral mucosal bleeding. The patient was then given intravenous immunoglobulin (IVIG) 0.4 g/kg for 5 days, which was followed by an increased platelet count (96 $\times$ 10^9 L^{-1}). Splenectomy was performed, but her platelet count fell

quickly to $10 \times 10^9\ L^{-1}$. She was treated, successively, with *Helicobacter pylori* eradication, danazol, azathoprine, and cyclosporine, but her platelets remained $<10 \times 10^9\ L^{-1}$, and she required weekly platelet transfusions. In August 2003, we tried rituximab at a dose of 375 mg/m^2 weekly for 4 doses. The patient's platelet count rose to $>100 \times 10^9\ L^{-1}$ within 5 weeks and remained at this level for 9 weeks thereafter. However, she relapsed 13 weeks after the rituximab treatment, and was again transfusion-dependent, despite treatment with high-dose dexamethasone (40 mg for 4 days), prednisolone (1 mg/kg), vincristine, danazol, and azathioprine. She received a second rituximab therapy in December 2003, which resulted in a partial platelet response (platelets $30–50 \times 10^9\ L^{-1}$) that eliminated the need for platelet transfusion. A monthly pulse cyclophosphamide (300–500 mg) was added, and the patient's platelet count remained $>50 \times 10^9\ L^{-1}$ for the next 10 months. In November 2004, the patient developed gastrointestinal bleeding and her platelet count was $<10 \times 10^9\ L^{-1}$, requiring IVIG treatment and platelet transfusion. A third rituximab treatment was given in March 2005, but there was no platelet response. Since then, she has received biweekly IVIG (a single dose of 0.4 g/kg) to maintain a safe platelet count.

Immunologic analyses

Platelet-associated IgG anti-GPIIb/IIIa antibodies and circulating IgG anti-GPIIb/IIIa antibody-producing cells were measured using, respectively, an enzyme-linked immunosorbent assay (ELISA) [10] and an enzyme-linked immunospot (ELISPOT) assay [11]. Human antichimeric antibodies (HACA) were measured using ELISA [12]. Flow cytometric analysis was performed using the following mouse monoclonal antibodies, which were conjugated to fluorescein isothiocyanate, phycoerythrin, or allophycocyanin: anti-CD3, anti-CD138 (Beckman Coulter, Fullerton, CA), anti-CD19 (Sigma, St. Louis, MO), anti-CD20 (BD Biosciences, San Diego, CA), and anti-CD34 (Miltenyi Biotech, Bergisch Gladbach, Germany). Negative controls were cells incubated with an isotype-matched mouse monoclonal antibody to an irrelevant antigen. The cells were analyzed on an FACS® Calibur flow cytometer (BD Biosciences) using CellQuest software. In some experiments, peripheral blood mononuclear cells (PBMC) depleted of $CD19^+$, $CD20^+$, $CD138^+$, or $CD34^+$ cells were used for the ELISPOT assay. The cell depletion was performed using magnetic bead-coupled anti-CD19, anti-CD20, or anti-CD34 monoclonal antibodies (Miltenyi Biotech) or anti-CD138 monoclonal antibody (Beckman Coulter) in combination with magnetic bead-coupled anti-mouse IgG antibodies (Miltenyi Biotech), followed by separation on a MACS column. Flow cytometric analysis revealed that cells positive for corresponding markers were nearly absent in the treated fractions (<0.5% for $CD19^+$ and $CD20^+$ cells, and <0.01% for $CD138^+$ and $CD34^+$ cells).

Acknowledgment

We thank Yuka Okazaki for excellent technical assistance.

References

1. Cines DB, Blanchette V. Immune thrombocytopenic purpura. New Engl J Med 2002;346:995–1008.
2. George J. Management of patients with refractory immune thrombocytopenic purpura. J Thromb Haemost 2006;4:1664–1672.
3. Maloney DG, Liles TM, Czerwinski DK, et al. Phase I clinical trial using escalating single-dose infusion of chimeric anti-CD20 monoclonal antibody (IDEC-C2B8) in patients with recurrent B-cell lymphoma. Blood 1994;84:2457–2466.
4. Cooper N, Stasi R, Cunningham-Rundles S, et al. The efficacy and safety of B-cell depletion with anti-CD20 monoclonal antibody in adults with chronic immune thrombocytopenic purpura. Br J Haematol 2004;125:232–239.
5. Bennett CM, Rogers ZR, Kinnamon DD, et al. Prospective phase 1/2 study of rituximab in childhood and adolescent chronic immune thrombocytopenic purpura. Blood 2006;107:2639–2642.
6. Peñalver FJ, Jiménez-Yuste V, Almagro M, et al. Rituximab in the management of chronic immune thrombocytopenic purpura: An effective and safe therapeutic alternative in refractory patients. Ann Hematol 2006;85:400–406.
7. Herishanu Y. Rituximab-induced serum sickness. Am J Hematol 2002;70:329.
8. Maeda T, Yamada Y, Tawara M, et al. Successful treatment with a chimeric anti-CD20 monoclonal antibody (IDEC-C2B8, rituximab) for a patient with relapsed mantle cell lymphoma who developed a human anti-chimeric antibody. Int J Hematol 2001;74:70–75.
9. Hoyer BF, Manz RA, Radbruch A, Hiepe F. Long-lived plasma cells and their contribution to autoimmunity. Ann NY Acad Sci 2005;1050:124–133.
10. Kuwana M, Okazaki Y, Kaburaki J, Kawakami Y, Ikeda Y. Spleen is a primary site for activation of glycoprotein IIb-IIIa-reactive T and B cells in patients with immune thrombocytopenic purpura. J Immunol 2002;168:3675–3682.
11. Kuwana M, Okazaki Y, Kaburaki J, Ikeda Y. Detection of circulating B cells secreting platelet-specific autoantibody is a sensitive and specific test for the diagnosis of autoimmune thrombocytopenia. Am J Med 2003;114:322–325.
12. Reff ME, Carner K, Chambers KS, et al. Depletion of B cells in vivo by a chimeric mouse human monoclonal antibody to CD20. Blood 1994;83:435–445.

Excessive exposure to anionic surfaces maintains autoantibody response to β_2-glycoprotein I in patients with antiphospholipid syndrome

Yukie Yamaguchi,[1,2] Noriyuki Seta,[1] Junichi Kaburaki,[3] Kazuko Kobayashi,[4] Eiji Matsuura,[4] and Masataka Kuwana[1]

[1]Division of Rheumatology, Department of Internal Medicine, Keio University School of Medicine, Tokyo; [2]Department of Environmental Immuno-dermatology, Yokohama City University Graduate School of Medicine, Yokohama; [3]Department of Internal Medicine, Tokyo Electric Power Company Hospital, Tokyo; and [4]Department of Cell Chemistry, Okayama University Graduate School of Medicine, Dentistry and Pharmaceutical Sciences, Okayama, Japan

Antiphospholipid syndrome (APS) is an autoimmune prothrombotic disorder associated with autoantibodies to phospholipid (PL)–binding proteins, such as β_2-glycoprotein I (β_2GPI). We have recently reported that binding of β_2GPI to anionic PL facilitates processing and presentation of the cryptic β_2GPI epitope that activates pathogenic autoreactive T cells. To clarify mechanisms that induce sustained presentation of the dominant antigenic β_2GPI determinant in patients with APS, T-cell proliferation induced by β_2GPI-treated phosphatidylserine liposome (β_2GPI/PS) was evaluated in bulk peripheral blood mononuclear cell cultures. T cells from patients with APS responded to β_2GPI/PS in the presence of immunoglobulin G (IgG) anti-β_2GPI antibodies derived from APS plasma, and this response was completely inhibited either by the depletion of monocytes or by the addition of anti-FcγRI antibody. These findings indicate that efficient presentation of the cryptic determinants can be achieved by monocytes undergoing FcγRI-mediated uptake of β_2GPI-bound anionic surfaces in the presence of IgG anti-β_2GPI antibodies. Finally, β_2GPI-bound oxidized LDL or activated platelets also induced the specific T-cell response. Continuous exposure to these anionic surfaces may play a critical role in maintaining the pathogenic anti-β_2GPI antibody response in patients with APS. (Blood. 2007;110:4312-4318)

Introduction

Antiphospholipid syndrome (APS) is an autoimmune disorder characterized by arterial and venous thrombosis as well as recurrent intrauterine fetal loss in the presence of antiphospholipid antibodies.[1] β_2-glycoprotein I (β_2GPI) is the most common antigenic target recognized by the antiphospholipid antibodies, and anti-β_2GPI antibodies are shown to be strongly associated with thrombosis and other clinical manifestations of APS.[2-4] β_2GPI is a plasma protein that binds various anionic substances, including phospholipids (PLs), lipoproteins, and activated platelets and endothelial cells.[5-7] Several lines of evidence accumulated from animal models suggest that anti-β_2GPI antibodies are directly involved in the pathogenic processes of APS.[8,9]

We have recently identified CD4$^+$ T cells responsive to β_2GPI in patients with APS.[10-12] β_2GPI-reactive T cells can promote production of pathogenic immunoglobulin G (IgG) anti-β_2GPI antibodies from autologous B cells in vitro. These T cells respond to bacterially expressed recombinant β_2GPI fragments and chemically reduced β_2GPI, but fail to respond to native β_2GPI,[10] indicating that the epitopes recognized by β_2GPI-reactive T cells are cryptic determinants that are not generated through processing of native β_2GPI under normal circumstances. One of the major cryptic determinants recognized by β_2GPI-reactive T cells is the region spanning amino acids (AAs) 276-290, which contains the major PL-binding site at AA 281-288,[13,14] in the context of HLA-DRB4*0103 (DR53).[11] In our recent study employing β_2GPI-reactive CD4$^+$ T-cell clones generated from patients with APS, dendritic cells or macrophages pulsed with β_2GPI-bound phosphatidylserine (PS) liposome induced a response of T-cell clones specific for a peptide encoding AA 276–290 (p276-290) in HLA-DR–restricted and antigen-processing–dependent manners. In contrast, those pulsed with β_2GPI or PS liposome alone failed to induce a response.[15] Together these findings indicate that specialized antigen-presenting cells (APCs) capturing β_2GPI-coated anionic PLs efficiently present a disease-relevant cryptic T-cell determinant of β_2GPI as a result of antigen processing.

In patients with APS, anti-β_2GPI antibody levels are usually stable for many years. However, it remains unclear what mechanisms are responsible for the sustained presentation of the dominant cryptic β_2GPI determinant that activates β_2GPI-reactive T cells to subsequently produce pathogenic anti-β_2GPI antibodies. To elucidate these mechanisms, we examined the cellular and molecular factors required for the sustained activation of β_2GPI-reative T cells in patients with APS.

Patients, materials, and methods

Patients and controls

This study examined 5 patients, and all fulfilled the revised Sapporo criteria for APS proposed by the International Workshop.[16] These patients were selected based on the presence of DRB4*0103 (DR53), which is known to present a p276-290 peptide to T cells,[11] and positive IgG anti-β_2GPI antibody. The HLA class II alleles, including DRB1 and DRB4, were determined by restriction fragment length polymorphisms combined with

Submitted July 9, 2007; accepted August 23, 2007. Prepublished online as *Blood* First Edition paper, August 28, 2007; DOI 10.1182/blood-2007-07-100008.

An Inside *Blood* analysis of this article appears at the front of this issue.

The publication costs of this article were defrayed in part by page charge payment. Therefore, and solely to indicate this fact, this article is hereby marked "advertisement" in accordance with 18 USC section 1734.

locus-specific polymerase chain reaction using peripheral blood granulocyte-derived genomic DNA as a template.[17] IgG anti-β_2GPI antibody levels were measured with a commercial enzyme-linked immunosorbent assay (ELISA) kit (Yamasa, Choshi, Japan) using immobilized β_2GPI-cardiolipin complex as an antigen source. A commercial kit based on Russell viper venom test (Gradipore, Sydney, Australia) was used to determine the presence of lupus anticoagulant. At the time of blood examination, all the patients were taking low-dose corticosteroids (< 10 mg/day) and low-dose aspirin. Peripheral blood from healthy volunteers was also used as a control source of plasma. All samples were obtained after the patients and control subjects gave their written informed consent in accordance with the Declaration of Helsinki. The study protocol was approved by Keio University International Review Board.

Antigen preparations

Human β_2GPI was purified from normal pooled plasma,[18] and reduced β_2GPI was prepared by incubating β_2GPI with dithiothreitol as previously described.[10] We generated a panel of recombinant maltose-binding protein (MalBP) fusion proteins expressing full-length β_2GPI (GP-F), domains I and II (GP1), domains III and IV (GP2), and domains IV and V (GP3).[10] MalBP alone was prepared as a control antigen. Two 15-mer peptides, p276-290 and a peptide encoding AA 306–320 of human β_2GPI (p306-320), were synthesized using a solid-phase multiple synthesizer (Advanced ChemTech, Louisville, KY).[11]

Liposome containing bovine brain-derived PS (Sigma, St Louis, MO), with a composition of dioleoylphosphatidylcholine (Avanti Polar Lipids, Alabaster, AL) at a molar ratio of 3:7, was prepared and adjusted to a final concentration of 1 μmol/mL.[19,20] Low density lipoprotein (LDL) was isolated from freshly prepared normal human plasma by ultracentrifugation, and oxidized LDL (oxLDL) was prepared by incubating LDL with 5 μM $CuSO_4$ for 8 hours at 37°C.[20] LDL and oxLDL were adjusted to 100 μg/mL of apoB equivalent. Human platelets were separated from platelet-rich plasma using a modified gel filtration method[21] to minimize their activation during an isolation procedure. Resting platelets were then activated by incubation with bovine thrombin (1 U/mL; Mochida, Tokyo, Japan) for 15 minutes. All preparations were incubated with or without native β_2GPI (100 μg/mL) for 30 minutes at room temperature immediately prior to use in the cultures.

Cell preparations

Peripheral blood mononuclear cells (PBMCs) were isolated from heparinized venous blood by Lymphoprep (Fresenius Kabi Norge AS, Oslo, Norway) density-gradient centrifugation. In some experiments, PBMCs were depleted of $CD14^+$ monocytes or $CD19^+$ B cells by incubation with anti-CD14 or anti-CD19 monoclonal antibody (mAb)–coupled magnetic beads (Miltenyi Biotecch, Bergisch Gladbach, Germany), respectively, followed by magnetic cell sorting column separation according to the manufacturer's protocol.

Preparation and depletion of IgG from plasma

The IgG fraction was purified or depleted from plasma samples using HiTrap protein G (Amersham Biosciences, Uppsala, Sweden) as described previously.[22] Purity of IgG fractions was confirmed to be more than 95% by sodium dodecyl sulfate–polyacrylamide gel electropheresis, followed by densitometry on Coomassie blue–stained gels. In some experiments, purified IgG was treated with pepsin to prepare $F(ab')_2$ using a Fab2 preparation kit (Pierce Biotechnology, Rockford, IL). We also prepared IgG fractions depleted of antibodies specific to β_2GPI. Briefly, purified IgG samples were treated 3 times with cardiolipin-coated 96-well immunoplates (Nunc F96Maxisorp, Roskilde, Denmark), which were preincubated with β_2GPI or phosphate-buffer saline for 30 minutes. The supernatants were then collected as anti-β_2GPI antibody–depleted or mock-treated IgG. Removal of anti-β_2GPI antibody was confirmed by complete loss of antibody reactivity on the anti-β_2GPI antibody ELISA.

Assays for antigen-specific T-cell response

Antigen-specific T-cell proliferation in the primary cultures was assayed as described previously[10] with some modifications. Briefly, PBMCs (10^5/well) were cultured with or without antigen in 96-well flat-bottomed culture plates for 7 days. RPMI 1640 supplemented with either 10% fetal bovine serum (FBS; JRH Bioscience, Lenexa, KS) or 8% platelet-poor plasma, which was derived from patients with APS and healthy donors, was used as medium. Prior to use, FBS and plasma samples were heat-inactivated and depleted of β_2GPI by passing the samples through a HiTrap Heparin column (Amersham Biosciences) twice, to eliminate the potential influence of intrinsic β_2GPI on the generation of the antigenic peptides. ^{3}H-thymidine (0.5 μCi [0.0185 MBq]/well) was added to the cultures during the final 16 hours. The cells were harvested, and ^{3}H-thymidine incorporation was measured in a Top-Count microplate scintillation counter (Packard, Meriden, CT). Native β_2GPI, reduced β_2GPI, GP-F, GP1, GP2, GP3, and MalBP were used as antigens at a concentration of 10 μg/mL. In addition, PS liposome (0.1 μmol/mL), LDL, oxLDL (10 μg/mL apoB equivalent), resting platelets, or activated platelets (10^6/well) were added to the cultures, with or without preincubation with β_2GPI. To exclude nonspecific unresponsiveness of T cells, all experiments included a culture with phytohemagglutinin at a final concentration of 1 μg/mL. In some experiments, purified IgG, $F(ab')_2$, or anti-β_2GPI antibody–depleted or mock-treated IgG was added at the initiation of the culture. Anti-FcγRI (clone 10.1; R&D Systems, Minneapolis, MN), anti-HLA-DR (clone L243; Leinco Technologies, Baldwin, MO), or isotype-matched control mAb was also added to the culture at a final concentration of 2.5 μg/mL. All experiments were carried out in duplicate or triplicate, and the values are the mean counts per minute (cpm) plus or minus the standard deviation of multiple determinations. In some instances, a T-cell response specific to β_2GPI-treated PS liposome (β_2GPI/PS) was expressed as the ratio of cpm in the culture with β_2GPI/PS to cpm in the culture with PS liposome alone.

Secondary stimulation of peripheral blood T cells was also performed as described.[10] PBMCs were primed with β_2GPI/PS in medium supplemented with 8% autologous plasma for 10 days. Viable cells were then cultured for an additional 3 days in the presence of 50 U/mL recombinant interleukin-2 (Biogen Idec, San Diego, CA) and irradiated (3000 rad) autologous monocyte-derived dendritic cells in medium supplemented with 10% FBS in the absence or presence of β_2GPI, reduced β_2GPI, GP-F, GP1, GP2, GP3, MalBP (10 μg/mL), p276-290, or p306-320 (5 μg/mL). Frequencies of β_2GPI-reactive T cells in peripheral blood T cells were estimated by limiting dilution analysis using GP-F as an antigen.[23] The recognition of p276-290 by peripheral blood T cells was determined based on the specific response to p276-290 by at least 2 T-cell clones established by repeated stimulation of peripheral blood T cells with GP-F.[11]

Results

Clinical and immunologic characteristics of patients with APS

As shown in Table 1, all patients with APS had thrombosis and/or loss of pregnancy, and were positive for lupus anticoagulant. IgG anti-β_2GPI antibody titer was high in all but one patient (APS1). Frequencies of β_2GPI-reactive T cells were variable among patients, and ranged from 2.9 to 12.4 per 10^4 peripheral blood T cells. In addition, T-cell recognition of p276-290 was detected in all 3 patients examined.

T-cell response induced by β_2GPI/PS in PBMC cultures

We first examined the responses of peripheral blood T cells to β_2GPI/PS using regular medium supplemented with FBS (Figure 1A). T cells from all 5 patients responded to GP-F, but failed to proliferate in the presence of β_2GPI/PS. Interestingly, a T-cell response to β_2GPI/PS, as well as to GP-F, was detected when a patient's autologous plasma was used instead of FBS to supplement the culture medium. This response was blocked by anti–HLA-DR

Table 1. Clinical and immunologic characteristics of patients with APS analyzed in this study

Patient no.	Age/sex	Thrombosis	Loss of pregnancy	IgG anti-β_2GPI antibodies (U/mL)†	HLA class II alleles: DRB1	Frequency of β_2GPI-reactive T cells in circulation/10^4 T cells	Recognition of p276–290 by peripheral blood T cells
APS1	51/F	None	+	16	*1502/*0405	4.5	NT
APS2	43/F	DVT, stroke	+	>120	*0405/*1202	2.9	NT
APS3	46/F	DVT, PE, retinal artery thrombosis	+	>120	*1502/*0901	6.8	+
APS4	47/F	Stroke	+	>120	*1501/*0403	8.1	+
APS9	46/F	DVT, PE, stroke, amaurosis fugax	NA	>120	*0901	12.4	+

All patients were lupus anticoagulant positive; all DRB4 alleles were *0103.
DVT indicates deep venous thrombosis of lower extremity; PE, pulmonary embolism; NA, not applicable; and NT, not tested.
†Normal range less than 3.5 U/mL.

mAb, but not by control mAb (data not shown). However, a β_2GPI/PS-induced response was not detected in the culture with allogenic plasma from a healthy individual. This finding was reproducible in a total of 7 PBMC samples obtained from 5 patients with APS.

Next, PBMCs from a patient with APS were cultured with β_2GPI/PS or PS liposome alone in medium supplemented with 2 different lots of FBS, plasma samples from 4 patients with APS, or samples from 3 healthy donors (Figure 1B). The β_2GPI/PS-specific response was exclusively detected in cultures with autologous and allogenic plasmas derived from patients with APS, although the degree of response was variable among APS plasmas. Analogous findings were obtained with PBMCs from 3 additional patients with APS. In all cases, the lowest response was detected in the culture supplemented with APS1 plasma, which contained low-titer anti-β_2GPI antibodies.

We next sought to confirm whether T-cell responses induced by β_2GPI/PS in cultures with APS plasma were specific to β_2GPI. Peripheral blood T cells primed with β_2GPI/PS in medium supplemented with autologous plasma were further examined for their reactivity to various β_2GPI preparations in the secondary culture with FBS (Figure 2). β_2GPI/PS-primed T cells from all 5 patients specifically responded to reduced β_2GPI, GP-F, and GP3, indicating a specific recognition of β_2GPI-derived peptides. More important, the cryptic p276-290 was efficiently presented by APCs in culture with β_2GPI/PS and APS plasma. T-cell recognition of GP1 was detected in APS2, APS4, and APS9 samples, whereas recognition of GP2 was detected in APS3 and APS9. Taken together, these findings together indicate that a soluble factor(s) contained in plasma from patients with APS, but not in FBS or plasma from healthy individuals, plays an essential role in activation of β_2GPI-specific T cells in bulk PBMC cultures with β_2GPI/PS.

IgG anti-β_2GPI autoantibody as an essential factor for T-cell recognition of β_2GPI/PS

Since the degree of the β_2GPI/PS-specific T-cell response appeared to correlate with IgG anti-β_2GPI antibody titers, we hypothesized that IgG anti-β_2GPI antibodies in APS plasma are required for peripheral blood T cells to respond to β_2GPI/PS. To test this hypothesis, we first prepared IgG-depleted APS plasma samples to evaluate the β_2GPI/PS-induced T-cell response (Figure 3A). Depletion of IgG from APS plasma resulted in complete loss of the β_2GPI/PS-induced T-cell response, but addition of autologous IgG back to the IgG-depleted APS plasma restored the response in a dose-dependent fashion. In contrast, addition of IgG prepared from healthy plasma had no effect (data not shown). Interestingly, β_2GPI/PS-induced T-cell response was also detected in medium supplemented with healthy plasma in the presence of IgG derived from APS plasma. This response was abolished when $F(ab')_2$ was used instead of intact IgG, indicating an important role of the Fc portion of IgG.

We further examined the effects of depletion of β_2GPI-specific antibody on the β_2GPI/PS-induced T-cell response in PBMC cultures with APS IgG (Figure 3B). β_2GPI/PS-induced T-cell

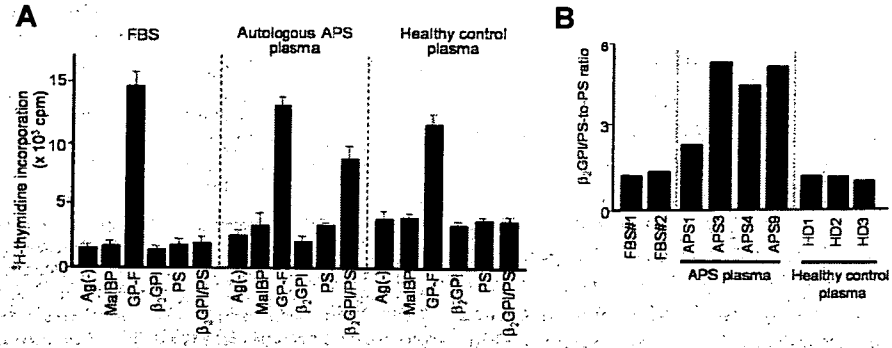

Figure 1. T-cell response to β_2GPI/PS in bulk PBMC cultures supplemented with FBS, autologous APS plasma, or healthy control plasma. (A) PBMCs from APS4 were cultured in triplicate with or without antigens, including MalBP, GP-F, β_2GPI, PS, and β_2GPI/PS, in medium supplemented with FBS, autologous APS plasma, or healthy control plasma. The antigen-induced T-cell proliferative response was assessed by ^{3}H-thymidine incorporation. Results are shown as mean (column) and standard deviation (error bar) of triplicate measurements. Analogous findings were obtained in 7 independent experiments in PBMCs from all 5 patients with APS. (B) β_2GPI/PS-specific T-cell response in PBMC cultures of APS4 in medium supplemented with 2 different lots of FBS (no. 1 and no. 2), plasma samples from 4 APS patients (APS1, 3, 4, and 9), or plasma samples from 3 healthy donors (HD1, 2, and 3). β_2GPI/PS-specific T-cell response was expressed as a β_2GPI/PS-to-PS ratio, which was the mean cpm incorporated in the triplicate culture with β_2GPI/PS divided by the mean cpm incorporated in the triplicate culture with PS alone (standard deviations for the individual results were within 20% of the mean in all cases). Similar results were obtained from 3 additional patients with APS (APS1, APS3, and APS9).

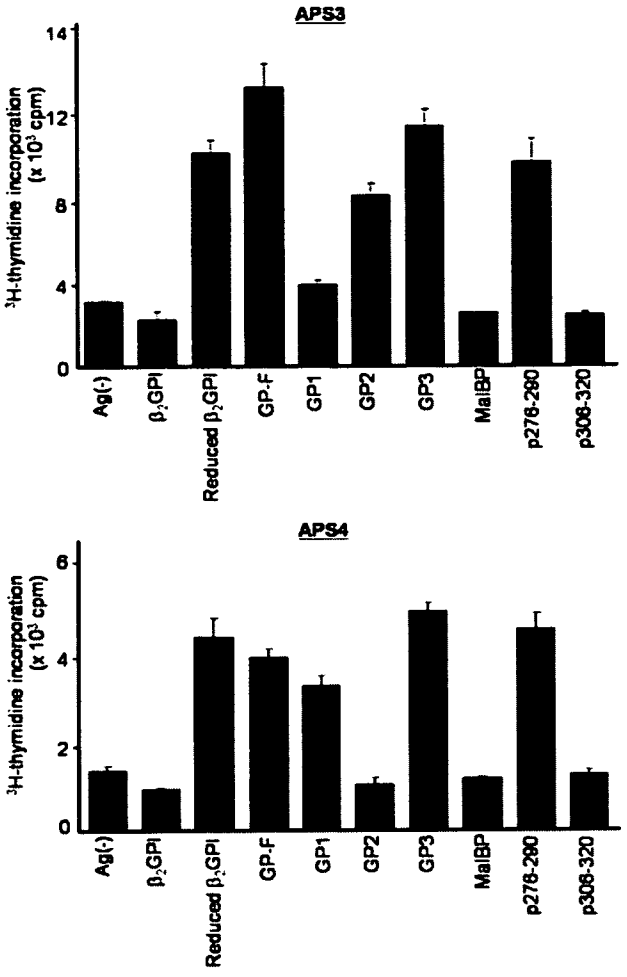

Figure 2. Proliferative responses of β_2GPI/PS-primed T cells to various β_2GPI preparations in secondary cultures. PBMCs from APS3 (top) and APS4 (bottom) were stimulated with β_2GPI/PS for 10 days in medium supplemented with autologous plasma. The viable T cells were then cultured in duplicate with β_2GPI, reduced β_2GPI, GP-F, GP1, GP2, GP3, MalBP, p276-290, or p306-320 in medium containing FBS. After 3 days, ^{3}H-thymidine incorporation was measured. Results are shown as mean (column) and standard deviation (error bar) of duplicate measurements.

response was detected in the presence of mock-treated APS IgG, but completely abolished by depletion of β_2GPI-reactive IgG. These findings indicate that IgG anti-β_2GPI antibodies are required for the T cells of patients with APS to respond to β_2GPI/PS in bulk PBMC cultures.

Roles of β_2GPI/PS-containing immune complex in β_2GPI/PS-induced T-cell response

Since anti-β_2GPI antibodies in sera from patients with APS recognize β_2GPI/PS,[20] it is likely that β_2GPI/PS is readily opsonized by IgG anti-β_2GPI antibodies in culture with APS plasma. To evaluate which APCs contained in PBMCs capture this immune complex to induce a specific T-cell response to β_2GPI peptides, we analyzed PBMCs depleted of CD14$^+$ monocytes, CD19$^+$ B cells, or mock-treated in cultures with β_2GPI/PS and autologous plasma (Figure 4A). The β_2GPI/PS-induced T-cell response was completely inhibited by depletion of monocytes, but was partially suppressed by depletion of B cells, suggesting a primary role of monocytes in our system.

We further evaluated the potential involvement of Fcγ receptors in recognition of the immune complex by monocytes, as the anti-β_2GPI F(ab')$_2$ was incapable of inducing the T-cell response to β_2GPI/PS. The β_2GPI/PS-induced T-cell response was completely blocked by anti-FcγRI mAb, but not by control mAb (Figure 4B). Together these findings indicate that efficient β_2GPI/PS-induced T-cell response is achieved by monocytes undergoing FcγRI-mediated uptake of β_2GPI/PS opsonized by IgG anti-β_2GPI autoantibodies.

T-cell response to β_2GPI-treated oxLDL and platelet microparticles

PS liposomes were chemically synthesized, and may not be relevant to patients with APS in vivo. To examine whether anionic substances present in the circulation, such as oxLDL or platelet microparticles, can substitute for PS liposomes in inducing the β_2GPI-specific T-cell response, PBMCs from a representative patient with APS were cultured with various anionic and control substances pretreated with or without β_2GPI in medium supplemented with autologous plasma (Figure 5). OxLDL or activated platelets pretreated with β_2GPI induced a T-cell proliferative

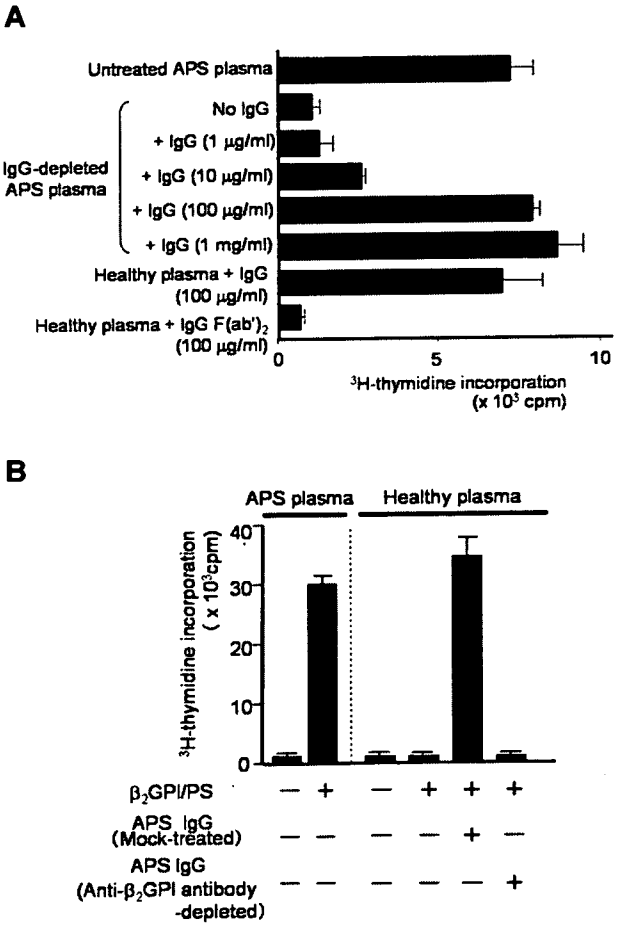

Figure 3. β_2GPI/PS-induced T-cell response in PBMC cultures with or without IgG derived from APS plasma. (A) PBMCs obtained from APS3 were cultured in triplicate with β_2GPI/PS in medium supplemented with untreated or IgG-depleted autologous APS plasma, or healthy plasma. Purified IgG (1 μg/mL-1 mg/mL) or IgG F(ab')$_2$ (100 μg/mL) from APS3 was added to the cultures. After 7 days, the T-cell proliferative response induced by β_2GPI/PS was measured by ^{3}H-thymidine incorporation. Results are shown as mean (column) and standard deviation (error bar). Concordant results were obtained with a sample from APS4. (B) PBMCs derived from APS3 were cultured in triplicate with or without β_2GPI/PS in medium supplemented with autologous APS plasma or healthy plasma. An anti-β_2GPI antibody–depleted or mock-treated autologous IgG fraction was added to the initiation of cultures. After 7 days, the T-cell proliferative response was measured by ^{3}H-thymidine incorporation. Results are shown as mean (column) and standard deviation (error bar). Concordant results were obtained with a sample from APS4.

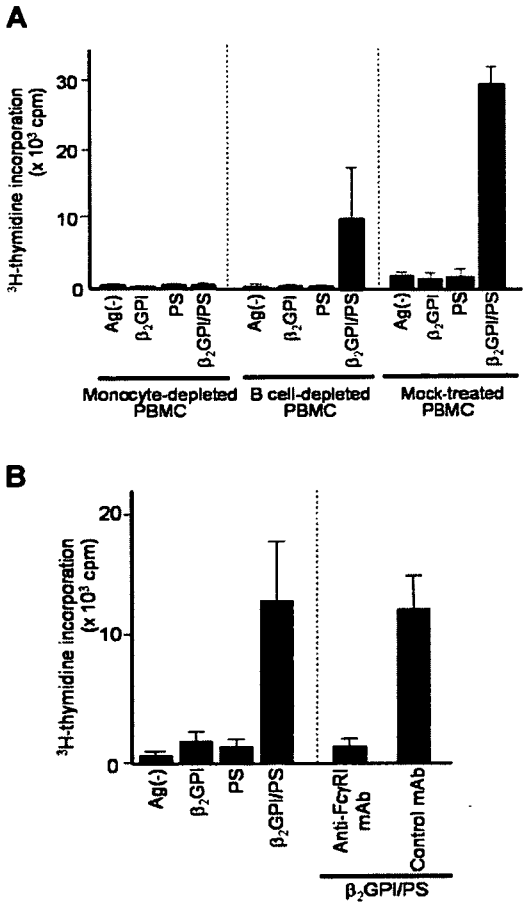

Figure 4. Effects of APC depletion or anti-FcγRI mAb on β_2GPI/PS-induced T-cell response. (A) CD14$^+$ monocyte-depleted, CD19$^+$ B-cell–depleted, and mock-treated PBMCs derived from APS3 were cultured for 7 days with or without β_2GPI, PS, or β_2GPI/PS in medium supplemented with autologous APS plasma, and the T-cell proliferative response was measured by ^{3}H-thymidine incorporation. Results are shown as mean (column) and standard deviation (error bar) of duplicate measurements. Analogous results were obtained in a total of 4 independent experiments using samples from 3 patients with APS (APS1, APS3, and APS4). (B) PBMCs from APS2 were cultured for 7 days with or without β_2GPI, PS, or β_2GPI/PS in medium supplemented with autologous APS plasma. Anti-FcγRI or isotype-matched control mAb was added to the initiation of cultures. The T-cell proliferative response was evaluated by ^{3}H-thymidine incorporation. Results are shown as mean (column) and standard deviation (error bar) of duplicate measurements. Concordant results were obtained with samples from 3 patients with APS (APS2, APS3, and APS9).

response, as observed in cultures with β_2GPI/PS. These responses were specifically inhibited by anti–HLA-DR mAb (data not shown). Thus, oxLDL and activated platelets can be in vivo sources of anionic surfaces that bind β_2GPI and promote the efficient presentation of β_2GPI cryptic peptides by APCs.

Discussion

This study evaluated the potential cellular and molecular mechanisms that induce sustained presentation of the dominant cryptic β_2GPI determinant that activates β_2GPI-reactive T cells to subsequently produce pathogenic anti-β_2GPI antibodies in patients with APS. Here we demonstrate that efficient presentation of cryptic determinants recognized by β_2GPI-reactive T cells is achieved by monocytes undergoing FcγRI-mediated uptake of β_2GPI/PS opsonized by IgG anti-β_2GPI antibodies. High avidity IgG anti-β_2GPI antibodies, which were reported to possess high pathogenicity,[24] would also have enhanced capacity to promote this process. We

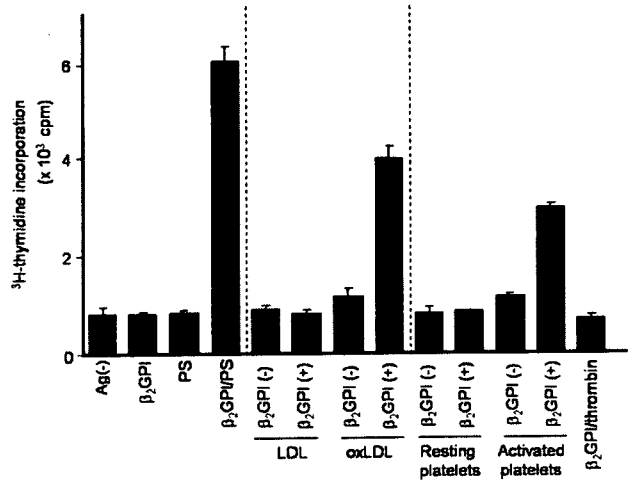

Figure 5. T-cell responses to β_2GPI-treated anionic substances present in circulation. PBMCs from APS4 were cultured with or without various antigen preparations in medium supplemented with autologous APS plasma. Antigens used included β_2GPI alone, as well as PS, LDL, oxLDL, resting platelets, and activated platelets, which were treated either with or without β_2GPI. Thrombin, which was used to activate platelets, in combination with β_2GPI served as a control. T-cell proliferative response was measured by ^{3}H-thymidine incorporation. Results are shown as mean (column) and standard deviation (error bar) of duplicate measurements. Analogous results were obtained in samples from all 5 patients with APS.

propose a model by which a pathogenic loop maintains sustained anti-β_2GPI autoantibody production in patients with APS (Figure 6). This model consists of 3 major players: β_2GPI-reactive CD4$^+$ T cells, anti-β_2GPI antibody-producing B cells, and macrophages. Upon recognition of β_2GPI cryptic peptides, such as p276-290, presented by macrophages in the context of HLA-DR, β_2GPI-reactive CD4$^+$ T cells are activated and exert helper activity that induces IgG anti-β_2GPI antibody production from B cells. This process can be achieved by T-B cell collaboration through CD40-CD154 engagement and T cell–derived IL-6.[11] IgG anti-β_2GPI antibodies subsequently recognize β_2GPI-bound anionic surfaces in circulation, resulting in enhanced phagocytosis of this immune

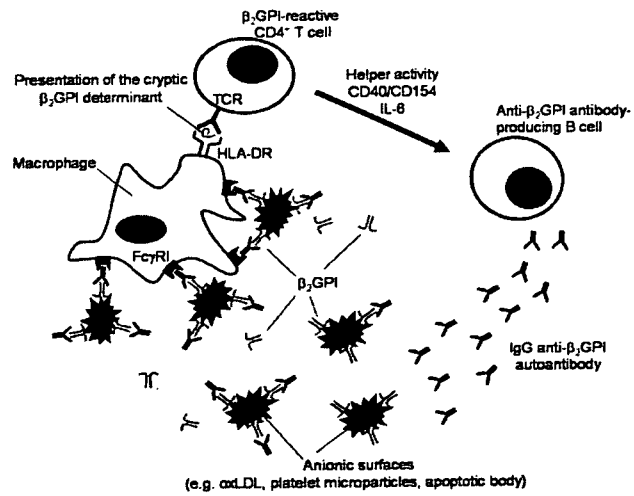

Figure 6. A schematic model representing a continuous autoimmune loop carried out by macrophage, β_2GPI-reactive CD4$^+$ T cell, and anti-β_2GPI antibody–producing B cell. The macrophage efficiently presents the cryptic β_2GPI determinant in the context of HLA-DR. The β_2GPI-reactive CD4$^+$ T cell is activated by recognition of the cryptic β_2GPI peptide and exerts helper activity that induces production of IgG anti-β_2GPI autoantibodies from the specific B cell. The immune complex consisting of anionic surfaces, β_2GPI, and IgG anti-β_2GPI antibodies were captured by macrophages via FcγRI.

complex by macrophages through FcγRI. In this regard, it has been shown that anti-β_2GPI antibodies in APS sera are predominantly of IgG2 subclass,[25,26] which has low affinity to FcγRI. However, anti-β_2GPI antibodies of IgG1 or IgG3 subclass were also detected in many patients with APS. These low levels of anti-β_2GPI antibodies with high binding affinity to FcγRI may be sufficient to drive the pathogenic loop. We have previously shown that β_2GPI binding to anionic substances promotes the generation of β_2GPI cryptic peptides by protecting the major PL-binding site from protease attack during antigen-processing by dendritic cells or macrophages.[15] Since it has been shown that antibody binding to the antigen boosts the generation of some minor epitopes,[27] binding of IgG anti-β_2GPI antibodies to the β_2GPI-anionic substance complex may further amplify generation of previously cryptic β_2GPI peptides. Moreover, this immune complex is likely to stimulate monocytes via FcγRI to secrete tissue factor, which is shown to play an important role in thrombus formation in patients with APS.[28] Partial suppression of the β_2GPI/PS-induced T-cell response by depletion of B cells in our system suggests that presentation of cryptic β_2GPI peptides could be mediated through B cells that capture β_2GPI/PS via specific B-cell receptors. This process, however, might have less of an impact on the T-cell response, due likely to low abundance of specific B cells recognizing β_2GPI/PS. The mechanism that triggers anti-β_2GPI antibody response in patients with APS remains unclear, but once this autoimmune loop is established, pathogenic anti-β_2GPI antibodies are continuously produced.

The presence of anionic substances with the capacity to bind β_2GPI is essential to drive the pathogenic loop inducing continuous anti-β_2GPI antibody production in patients with APS. Potential anionic substances in the circulation include apoptotic bodies, microparticles derived from activated platelets and endothelial cells, and oxLDL. Since β_2GPI is abundantly present in the circulation (~200 μg/mL), excessive exposure to anionic substances would result in the immediate formation of a complex with β_2GPI. In the present study, we have clearly demonstrated that microparticles derived from activated platelets and oxLDL can function as a substitute for the PS liposome that binds to β_2GPI and facilitates presentation of the cryptic epitopes of β_2GPI as a consequence of antigen processing. In addition, some of our group (E.M. and K.K.) reported that stable and nondissociable β_2GPI-oxLDL complexes were frequently detected in sera from patients with APS and/or systemic lupus erythematosus, but not in healthy individuals.[29] In addition, β_2GPI is known to have antiatherosclerosis activity by preventing oxLDL uptake by macrophages via scavenger receptor, but binding of IgG anti-β_2GPI antibodies to β_2GPI-oxLDL complexes mediates atherosclerosis by promoting phagocytosis of macrophages via Fcγ receptor.[29-31] Furthermore, elevated levels of procoagulant microparticles were detected in patients with APS in association with anti-β_2GPI antibodies and lupus anticoagulant.[32-34] The presence of a large quantity of anionic substances in circulation in patients with APS supports our proposed model.

Based on our model, therapeutic strategies that inhibit pathogenic anti-β_2GPI antibody production should target interrupting the continuous autoimmune loop carried out by macrophages and β_2GPI-reactive CD4$^+$ T cells and B cells. These immune cells are already targets of therapies under consideration, such as the anti-CD20 chimeric antibody rituximab.[35] Another potential therapeutic approach includes the removal of immune complexes consisting of β_2GPI, anionic substance, and anti-β_2GPI antibodies. Accordingly, plasma exchange and double filtration plasmapheresis, which theoretically remove such immune complexes, are shown to be effective for patients with intractable APS, including catastrophic APS.[36,37] Alternatively, small molecules that inhibit Fc receptor downstream signaling would have beneficial effects in patients with APS by suppressing the generation of β_2GPI cryptic peptides.[38]

In summary, excessive exposure to anionic surfaces may play a key role in maintaining the pathogenic anti-β_2GPI antibody response in patients with APS. Further studies should focus on mechanisms that prime the autoimmune loop and development of novel therapeutic strategies targeting the pathogenic process.

Acknowledgments

We thank Yuka Okazaki and Takahide Arai for expert technical assistance.

This work was supported by a grant from the Japanese Ministry of Health, Welfare, and Labor, and a Grant-in-Aid for Scientific Research from the Japanese Ministry of Education, Science, Sports and Culture.

Authorship

Contribution: Y.Y., N.S., J.K., K.K., and E.M. performed experiments; Y.Y. and M.K. analyzed results and made the figures; Y.Y. and M.K. designed the research and wrote the paper.

Conflict-of-interest disclosure: The authors declare no competing financial interests.

Correspondence: Masataka Kuwana, Division of Rheumatology, Department of Internal Medicine, Keio University School of Medicine, 35 Shinanomachi, Shinjuku-ku, Tokyo 160-8582, Japan; e-mail: kuwanam@sc.itc.keio.ac.jp.

References

1. Harris EN, Chan JK, Asherson RA, Aber VR, Gharavi AE, Hughes GRV. Thrombosis, recurrent fetal loss, and thrombocytopenia: predictive value of the anticardiolipin antibody test. Arch Intern Med. 1986;146:2153-2156.
2. McNeil HP, Simpson RJ, Chesterman CN, Krilis SA. Antiphospholipid antibodies are directed against a complex antigen that includes a lipid-binding inhibitor of coagulation: β_2-glycoprotein I (apolipoprotein H). Proc Natl Acad Sci U S A. 1990;87:4120-4124.
3. Galli M, Comfurius P, Maassen C, et al. Anticardiolipin antibodies (ACA) directed not to cardiolipin but to a plasma protein cofactor. Lancet. 1990;335:1544-1547.
4. Cabral AR, Amigo MC, Cabiedes J, Alarcon-Segovia D. The antiphospholipid/cofactor syndromes: a primary variant with antibodies to β_2-glycoprotein-I but no antibodies detectable in standard antiphospholipid assays. Am J Med. 1996;101:472-481.
5. Wurm H. β_2-glycoprotein I (apolipoprotein H) interactions with phospholipid vesicles. Int J Biochem. 1984;16:511-515.
6. Shi W, Chong BH, Chesterman CN. β_2-glycoprotein I is a requirement for anticardiolipin antibodies binding to activated platelets: differences with lupus anticoagulant. Blood. 1993;81:1255-1262.
7. Del Papa N, Guidali L, Sala A, et al. Endothelial cells as target for antiphospholipid antibodies: human polyclonal and monoclonal anti β_2-glycoprotein I antibodies react in vitro with endothelial cells through adherent β_2-glycoprotein I and induce endothelial activation. Arthritis Rheum. 1997;40:551-561.
8. Blank M, Faden D, Tincani A, et al. Immunization with anticardiolipin cofactor (β_2-glycoprotein I) induces experimental antiphospholipid syndrome in naive mice. J Autoimmun. 1994;7:441-455.
9. Levy Y, Ziporen L, Gilburd B, et al. Membranous nephropathy in primary antiphospholipid syndrome: description of a case and induction of renal injury in SCID mice. Hum Antibodies Hybridomas. 1996;7:91-96.

10. Hattori N, Kuwana M, Kaburaki J, Mimori T, Ikeda Y, Kawakami Y. T cells that are autoreactive to β_2-glycoprotein I in patients with antiphospholipid syndrome and healthy individuals. Arthritis Rheum. 2000;43:65-75.
11. Arai T, Yoshida K, Kaburaki J, et al. Autoreactive CD4+ T-cell clones to β_2-glycoprotein I in patients with antiphospholipid syndrome: preferential recognition of the major phospholipid-binding site. Blood. 2001;98:1889-1896.
12. Yoshida K, Arai T, Kaburaki J, Ikeda Y, Kawakami Y, Kuwana M. Restricted T-cell receptor β-chain usage by T cells autoreactive to β_2-glycoprotein I in patients with antiphospholipid syndrome. Blood. 2002;99:2499-2504.
13. Hunt J, Krilis SA. The fifth domain of β_2-glycoprotein I contains a phospholipid binding site (Cys281-Lys288) and a region recognized by anticardiolipin antibodies. J Immunol. 1994;152:653-659.
14. Sheng Y, Sali A, Herzog H, Lahnstein J, Krilis SA. Site-directed mutagenesis of recombinant human β_2-glycoprotein I identifies a cluster of lysine residues that are critical for phospholipid binding and anti-cardiolipin antibody activity. J Immunol. 1996; 157:3744-3751.
15. Kuwana M, Matsuura S, Kobayashi K, et al. Binding of β_2-glycoprotein I to anionic phospholipids facilitates processing and presentation of a cryptic epitope that activates pathogenic autoreactive T cells. Blood. 2005;105:1552-1557.
16. Miyakis S, Lockshin MD, Atsumi T, et al. International consensus statement on an update of the classification criteria for definite antiphospholipid syndrome (APS). J Thromb Haemost. 2006;4: 295-306.
17. Naruse T, Ando R, Nose Y, et al. HLA-DRB4 genotyping by PCR-RFLP: diversity in the associations between HLA-DRB4 and DRB1 alleles. Tissue Antigens. 1997;49:152-159.
18. Matsuura E, Igarashi Y, Fujimoto M, et al. Heterogeneity of anticardiolipin antibodies defined by the anticardiolipin cofactor. J Immunol. 1992;148: 3885-3891.
19. Liu Q, Kobayashi K, Furukawa J, et al. ω-Carboxyl variants of 7-ketocholesteryl esters are ligands for β_2-glycoprotein I and mediate antibody-dependent uptake of oxidized LDL by macrophages. J Lipid Res. 2002;43:1486-1495.
20. Kobayashi K, Matsuura E, Liu Q, et al. A specific ligand for β_2-glycoprotein I mediates autoantibody-dependent uptake of oxidized low density lipoprotein by macrophages. J Lipid Res. 2001; 42:697-709.
21. Bogdan W, Urszula K, Lidia M, et al. Comparison of platelet aggregability and P-selectin surface expression on platelets isolated by different methods. Thromb Res. 2000;99:495-502.
22. Nakamura M, Tanaka Y, Satoh T, et al. Autoantibody to CD40 ligand in systemic lupus erythematosus: association with thrombocytopenia but not thromboembolism. Rheumatology (Oxford). 2006;45: 150-156.
23. Kuwana M, Okazaki Y, Kaburaki J, et al. Spleen is a primary site for activation of platelet-reactive T and B cells in patients with immune thrombocytopenic purpura. J Immunol. 2002;168:3675-3682.
24. Božič B, Čučnik T, Kveder T, Rozman B. Avidity of anti-beta-2-glycoprotein I antibodies. Autoimmunity Rev. 2005;4:303-308.
25. Samarkos M, Davies KA, Gordon C, Walport MJ, Loizou S. IgG subclass distribution of antibodies against β_2-GPI and cardiolipin in patients with systemic lupus erythematosus and primary antiphospholipid syndrome, and their clinical associations. Rheumatology (Oxford). 2001;40:1026-1032.
26. Amengual O, Atsumi T, Khamashta MA, Bertolaccini ML, Hughes GRV. IgG2 restriction of anti-β_2-glycoprotein I as the basis for the association between IgG2 anticardiolipin antibodies and thrombosis in the antiphospholipid syndrome. Arthritis Rheum. 1998;41:1513-1514.
27. Simitsek PD, Campbell DG, Lanzavecchia A, Fairweather N, Watts C. Modulation of antigen processing by bound antibodies can boost or suppress class II major histocompatibility complex presentation of different T cell determinants. J Exp Med. 1995;181:1957-1963.
28. Wolberg AS, Roubey RAS. Mechanisms of autoantibody-induced monocyte tissue factor expression. Thromb Res. 2004;114:391-396.
29. Kobayashi K, Kishi M, Atsumi T, et al. Circulating oxidized LDL forms complexes with β_2-glycoprotein I: implication as an atherogenic autoantigen. J Lipid Res. 2003;44:716-726.
30. Matsuura E, Kobayashi K, Koike T, Shoenfeld Y. Autoantibody-mediated atherosclerosis. Autoimmunity Rev. 2002;1:348-353.
31. Shoenfeld A, Gerli R, Doria A, et al. Accelerated atherosclerosis in autoimmune rheumatic diseases. Circulation. 2005;112:3337-3347.
32. Morel O, Jesel L, Freyssinet JM, Toti F. Elevated levels of procoagulant microparticles in a patient with myocardial infarction, antiphospholipid antibodies and multifocal cardiac thrombosis. Thromb J. 2005;3:15.
33. Ambrozic A, Bozic B, Kveder T, et al. Budding, vesiculation and permeabilization of phospholipid membranes-evidence for a feasible physiologic role of beta2-glycoprotein I and pathogenic actions of anti-beta2-glycoprotein I antibodies. Biochim Biophys Acta. 2005;1740:38-44.
34. Combes V, Simon AC, Grau GE, et al. In vitro generation of endothelial microparticles and possible prothrombotic activity in patients with lupus anticoagulant. J Clin Invest. 1999;104:93-102.
35. Rubenstein E, Arkfeld DG, Metyas S, Shinada S, Ehresmann S, Liebman HA. Rituximab treatment for resistant antiphospholipid syndrome. J Rheumatol. 2006;33:355-357.
36. Cervera R, Font J, Gomez-Puerta JA, et al. Validation of the preliminary criteria for the classification of catastrophic antiphospholipid syndrome. Ann Rheum Dis. 2005;64:1205-1209.
37. Otsubo S, Nitta K, Yumura W, Nihei H, Mori N. Antiphospholipid syndrome treated with prednisolone, cyclophosphamide and double-filtration plasmapheresis. Intern Med. 2002;41:725-729.
38. Braselmann S, Taylor V, Zhao H, et al. R406, an orally available spleen tyrosine kinase inhibitor blockes Fc receptor signaling and reduces immune complex-mediated inflammation. J Pharmacol Exp Ther. 2006;319:998-1008.

A large deletion of the *PROS1* gene in a deep vein thrombosis patient with protein S deficiency

Tong Yin[1], Satoshi Takeshita[2], Yukiko Sato[1], Toshiyuki Sakata[3], Yongchol Shin[1], Shigenori Honda[1], Tomio Kawasaki[4], Hajime Tsuji[5], Tetsuhito Kojima[6], Seiji Madoiwa[7], Yoichi Sakata[7], Mitsuru Murata[8], Yasuo Ikeda[9], Toshiyuki Miyata[1]

[1]Research Institute, [2]Department of Medicine and [3]Laboratory for Clinical Chemistry, National Cardiovascular Center, Osaka, Japan; [4]Department of Surgery, Graduate School of Medicine, Osaka University, Osaka, Japan; [5]Division of Blood Transfusion and Cell Therapy, Kyoto Prefectural University of Medicine, Kyoto, Japan; [6]Department of Medical Technology, Nagoya University of School of Health Sciences, Nagoya, Japan; [7]Division on Cell and Molecular Medicine, Center for Molecular Medicine, Jichi Medical School, Shimotsuke, Tochigi, Japan; Departments of [8]Laboratory Medicine and [9]Internal Medicine, Keio University, Tokyo, Japan

Summary

Inherited deficiency of protein S encoded by the *PROS1* gene constitutes an important risk factor for deep vein thrombosis (DVT). Nevertheless, although more than 200 deleterious genetic variations in *PROS1* have been identified, causative point mutations of *PROS1* gene are not detected in approximately half of protein S-deficient families. The present study investigated whether there may exist a large deletion in *PROS1* that constitutes a genetic risk factor for Japanese DVT patients. A multiplex ligation-dependent probe amplification analysis was employed to identify the deletions in *PROS1* in 163 Japanese patients with DVT. A large gene deletion was identified in one patient who showed 16% protein S activity and did not carry point mutations in *PROS1* by DNA sequencing and it was validated by the quantitative PCR method. The deletion spanned at least the whole *PROS1* gene (107 kb) and at most from the centromere located downstream of *PROS1*, to before the D3S3619 marker, the first heterozygous marker in the upstream of *PROS1* in chromosome 3. In conclusion, a large deletion in *PROS1* was shown to partly account for DVT with protein S deficiency. Screening for large deletions in *PROS1* might be warranted in *PROS1* causative point mutation-negative DVT patients with protein S deficiency.

Keywords

Gene deletion, deep vein thrombosis, protein S deficiency, *PROS1*, MLPA

Thromb Haemost 2007; 98: 783–789

Introduction

Imbalance between procoagulant and anticoagulant potencies triggers coagulation. Protein S (PS) is a cofactor for the anticoagulant protease, activated protein C (PC), which proteolytically inactivates activated coagulation factors V and VIII. Therefore, inherited deficiency of PS constitutes an important risk factor for venous thrombosis (1). In the general Japanese population, PS deficiency is relatively common, and its estimated prevalence, 1.12%, is much higher than that in the Caucasian population (0.16–0.21%) (2–4). Recently, we and others identified a PS K196E mutation (PS Tokushima) as a genetic risk factor for the development of deep vein thrombosis (DVT) (5–8).

The gene for PS (*PROS1*) is located near the centromere on chromosome 3. It spans approximately 101 kb of genomic DNA and comprises 15 exons and 14 introns (9–12). Human DNA contains the active *PROS1* gene at 3q11.2 and a closely linked pseudogene (*PROSP*) at 3p21-cen that shows 96.5% homology to exons 2 to 15 of the *PROS1* gene. To date, more than 200 deleterious mutations in the *PROS1* gene have been reported (13). Most of the gene defects are small point mutations, such as missense, nonsense, frameshift, or splice site mutations, which are

Correspondence to:
Toshiyuki Miyata, PhD
Department of Etiology and Pathogenesis
National Cardiovascular Center Research Institute
5-7-1 Fujishirodai, Suita, Osaka 5658565, Japan
Tel.: +81 66833 5012, Fax: +81 66835 1176
E-mail: miyata@ri.ncvc.go.jp

Financial support:
This study was supported by the Program for Promotion of Fundamental Studies in Health Sciences of the National Institute of Biomedical Innovation (NIBIO) of Japan, a Grant-in-Aid from the Ministry of Health, Labor, and Welfare of Japan, and the Ministry of Education, Culture, Sports, Science, and Technology of Japan. Tong Yin, M.D., is a recipient of Takeda Foundation, from Institute of Geriatric Cardiology, General Hospital of People's Liberation Army, Beijing, China.

Received March 21, 2007
Accepted after resubmission July 25, 2007

Prepublished online September 10, 2007
doi:10.1160/TH07-03-0211

scattered throughout the coding region of the *PROS1* gene. Some studies have reported that causative point mutations in *PROS1* were found only in approximately 50% of the cases with functional low PS activity (14). One possible cause of such PS deficiency is the existence of large deletions or inversions covering all or part of the *PROS1* gene, which are difficult to identify by current PCR-based sequencing methods. Several studies in PS-deficient families with *PROS1* causative point mutation-negative members indicated that large deletions of *PROS1* have been identified in patients with PS deficiency and screening for large deletions in *PROS1* causative point mutation-negative individuals is therefore warranted (15–18).

A wide range of methods are available for gene dosage measurement to detect large deletions or insertions, but no one method offers overwhelming advantages. Recently developed technique, multiplex ligation-dependent probe amplification (MLPA), based on PCR amplification of ligated probes hybridized to the target DNA (19, 20), would be beneficial for detecting large cryptic genetic variations. This method has proven to be accurate and reliable for identifying deletions, duplications, and amplifications in several diseases (21–23). In this study, we utilized the MLPA method to determine whether there might be large deletions in *PROS1* that constitute genetic risk factors for DVT in Japanese patients.

Materials and methods

Patients

One hundred sixty-three DVT patients, 78 men and 85 women, were registered by the Study Group of Research on Measures for Intractable Diseases, working under the auspices of the Ministry of Health, Labor, and Welfare of Japan. Six centers (one each in Tochigi, Tokyo, Nagoya, and Kyoto, and two in Osaka) participated in this study (5). The protocol for the study was approved by the ethical review committee, and only those subjects who provided written informed consent for genetic analysis were included.

Clinical profile of a patient with a large *PROS1* gene deletion

A previously healthy 22-year-old female was admitted to our hospital due to swelling of her left limb for the past two months. She had no family history of thrombotic diseases. On physical examination, she showed no abnormal findings except swelling of the left thigh and calf.

Laboratory examination showed that the levels of free PS antigen and PS activity had decreased to 2.1 μg/ml (normal range: 6.5–9.8 μg/ml) and 16% (normal range: 65–105%), respectively, while antithrombin (112.7%; normal range: 80–120%), PC (119%; normal range: 75–125%) and plasminogen (104.8%; normal range: 70–120%) were within the normal ranges. ^{99m}Tc-MAA scintigraphy revealed obstruction of the left common iliac and bilateral popliteal veins with no evidence of pulmonary embolisms. Because of the presence of DVT, decreased level of PS, and exclusion of other underlying diseases causing thrombosis, the patient was diagnosed with PS deficiency.

Laboratory values measurement

Some of the patients' plasma samples were stored at –80°C. We measured the PC amidolytic activity (24) and plasma PS activity using Staclot protein S (Diagnostica Stago, Asnieres, France) (3) in 34 samples of DVT patients.

MLPA method

MLPA was performed as described by Schouten et al. (19) using SALSA MLPA KIT P112 *PROS1* (MRC-Holland, Amsterdam, the Netherlands), a kit for screening deletions or duplications in the *PROS1* gene. The kit contains probes for 13 out of 15 exons in *PROS1*, one probe for the promoter located 6.5 kb upstream of *PROS1*, and one probe for exon 4 in *PROSP*. It also contains 17 control probes located on different chromosomes, 1p36, 2q14, 2q24, 3p22, 5q35, 7q31, 7q, 9p21, 10p12, 12p13, 12q14, 14q22, 15q21, 16q22, 18q21, 19p13, and 21q11. The ligation products were amplified by PCR using the common primer set with the 6-FAM label distributed by the supplier. Approximately 100 ng of genomic DNA was utilized for one MLPA reaction. Amplification products were run on an ABI PRISM 3130 DNA Sequencer with the GeneScan 500 LIZ size standard (Applied Biosystems, Foster City, CA, USA) and analyzed by GeneMapper Software 5.0 (Applied Biosystems).

Dosage analyses based on a comparison between deleted and reference wild-type DNA samples were performed on an Excel software Coffalyser V3 (MRC-Holland). Briefly, all *PROS1* peak areas were normalized by dividing each peak area by the combined areas of all the control probe peaks in the same sample. Then, these normalized peak areas were divided by the corresponding wild-type normalized peak areas (average of five independent normal DNA samples) of that probe amplification product, in order to obtain a series of patient-to-normal DNA copy number ratios. The MLPA analysis was repeated three times for all samples.

Q-PCR analysis

DNA copy numbers for 14 exons in *PROS1* and exon 4 in *PROSP* were determined by Q-PCR. Primers for each sequence (except for the sequence of exon 1) were designed to avoid concurrent amplification of the *PROSP* sequence. The amplicon length ranged from 67 to 198 bps. The PCR reaction and the reference genes were as described previously (25). Each assay included a no-template control (in duplex), 20 ng of normal calibrator human genomic DNA (Roche Applied Science, Indianapolis, IN, USA) (in quadruplicate), and 20 ng of sample DNA (in quadruplicate). Calculation of the gene copy number was performed using the comparative (delta-C_t) C_t method (26) and the Q-PCR automated analysis software package "qBase" (http://medgen.ugent.be/qbase/). A haploid copy number of 1 is expected for a normal sample and a value of ≤0.5 for a sample with deletion.

PROS1 sequence analysis

A genomic DNA sample from the DVT patient with the deletion in *PROS1* was sequenced for all exons in *PROS1* using an ABI 3730 sequencer (Applied Biosystems) (27). Genetic variations were identified with NAMIHEI (Mitsui Knowledge Industry Co., Ltd., Tokyo, Japan) and Sequencher (Gene Codes Corpor-

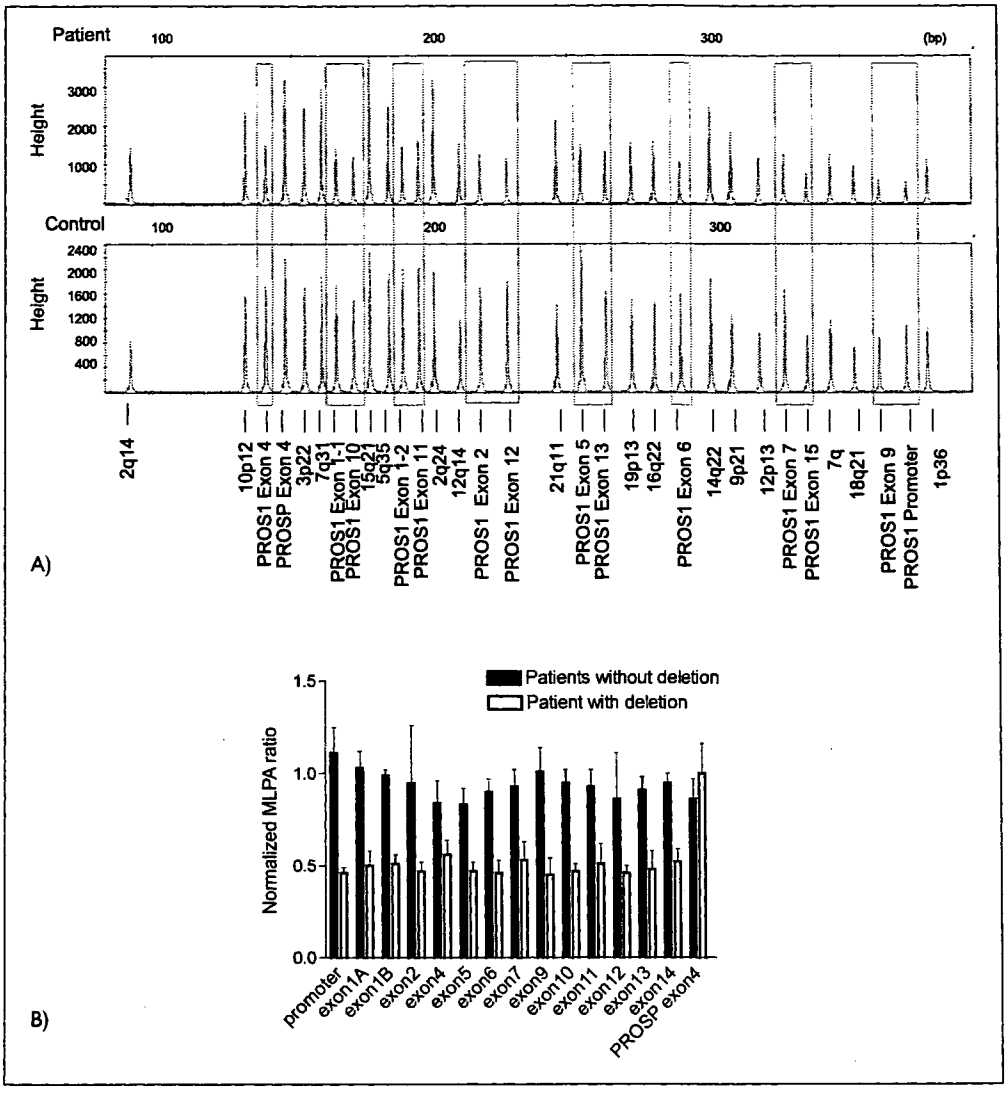

Figure 1: MLPA analysis of the deletion in the *PROS1* gene.
A) The representative MLPA electropherograms in one patient with the deletion in *PROS1* (top) and in a normal control DNA (bottom). Deleted exons are marked by squares. This is one representative of three rounds of MLPA analyses. Probes are 13 out of 15 exons in *PROS1* (two probes for exon 1), one probe for promoter located 6.5 kb upstream of *PROS1*, one probe for exon 4 in *PROSP* and 17 controls located on different chromosomes. B) The representative histograms showing a deletion of 14 probes in *PROS1* in one patient (white bars) and the average normalized MLPA ratio in the patients without deletion (black bars). The probe for exon 4 in *PROSP* is shown as the control probe. The data are presented as the means ± SD from three rounds of MLPA.

ation, Ann Arbor, MI, USA) software, followed by visual inspection (28).

SNPs genotyping and microsatellite analysis

Five SNP markers located within a 252 kb region centered on *PROS1* were chosen on the basis of the available data from NCBI Map Viewer (Build 36.2) and the genotyping of the markers was performed by the TaqMan-PCR genotyping system (29).

Four microsatellite markers (D3S3681, D3S1276, D3S3634 and D3S1271) covering a 22 Mbp region centered on the *PROS1* locus were obtained from the ABI Linkage Mapping Set Version 2.5 (Applied Biosystems), and the microsatellite marker analyses were performed according to the manufacturer's instructions. For the other five microsatellite markers (D3S3556, D3S1251, D3S3619, D3S1752 and D3S3716) in the region, we designed PCR primer sets. Primer sequences were available on request. PCR products were detected by Agilent Bioanalyzer 2100 (Agilent Technologies, Boeblingen, Germany) or by electrophoresis through the 12% polyacrylamide gel stained with SYBR Green I (Nucleic Acid Gel Stain (Molecular Probes, Eugene, OR, USA). The products were also directly sequenced to reveal the allele zygosity.

Results

Deletion detection using MLPA analysis

To identify the large deletions in *PROS1* in patients with DVT, we utilized MLPA analysis. This method has the advantage of using a relatively small amount of DNA – i.e. only 100 ng of genomic DNA are required for one MLPA analysis to reveal a *PROS1* gene deletion. A deletion of one copy of a probe target sequence is usually apparent by a 35–55% reduction in relative peak area. A gain in copy number from two to three copies is usually apparent by a 30–55% increase in relative peak area.

We identified reduced peak areas in the *PROS1* regions in one DVT patient, which indicates a heterozygous deletion encompassing the whole *PROS1* gene (Fig. 1). No significant changes were found in the peak areas of the control probes in-

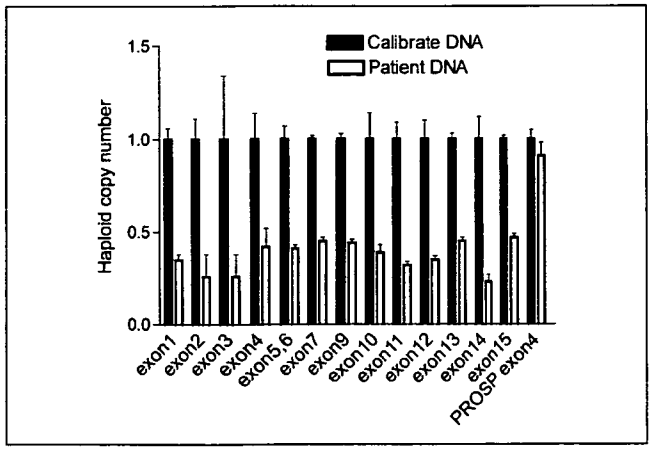

Figure 2: Haploid copy number status of *PROS1* determined by Q-PCR. Representative histogram showing the haploid copy numbers of *PROS1* exons in one patient with the *PROS1* deletion (white bars) and in the normally calibrated DNA (black bars). Data are presented as the means ± SD from Q-PCR reaction in quadruplicate. The copy number of *PROSP* exon 4 is plotted as no deletion control.

cluding *PROSP* exon 4 in this patient. For other patients, no reduced or increased peak areas were detected. The results of the MLPA analysis were reproducible, with three rounds of MLPA yielding identical findings in all patients. Based on the MLPA analysis, a minimum distance of *PROS1* deletion in this patient was estimated to be 107 kb between the *PROS1* promoter and exon 15 MLPA probes.

Deletion detection using Q-PCR

To confirm the deletions detected by MPLA in the patient, the patient's genomic DNA and a normally calibrated DNA were subjected to Q-PCR analysis to determine the copy numbers of *PROS1*. The analysis confirmed that all exons of *PROS1* were deleted in this patient (Fig. 2). No deletion was detected in *PROSP* exon 4.

Direct sequencing of the coding regions of *PROS1*

As described in *Methods*, PS antigen and PS activity of the patient with the deletion in *PROS1* decreased to 2.1 μg/ml (normal range: 6.5–9.8 μg/ml) and 16% (normal range: 65–105%), respectively, while antithrombin, PC and plasminogen were within normal ranges. This suggested that the patient might be a compound heterozygote for PS deficiency. To identify additional genetic variations in *PROS1* in the patient, we sequenced all exons of *PROS1* in this patient, but no point mutations were found.

Distribution of microsatellites and SNP genotypes

To define the range of deletions detected by the MLPA analysis, five SNP markers and nine microsatellite markers covering a 22 Mbp window centered on the *PROS1* locus were analyzed for their allele zygosities (Table 1). When the allele carries a deletion, it will be hemizygous for all markers within the deleted region, but will appear homozygous. Thus, if a specific marker is homozygous, there might be a deletion covering that locus, but if a specific marker is heterozygous, there must be no deletion covering that locus.

The five SNP markers flanking *PROS1* were homozygous. The marker D3S3619, which was located 1,949 kb upstream of *PROS1*, was detected as the first microsatellite heterozygosity in the upstream region of *PROS1* (Table 1). As a result, the boundary of the deletion in this patient must be within the range of D3S3619 to D3S1276. Since the centromere is located between *PROSP* and exon 15 of *PROS1*, one breakpoint of the deletion must be closer to exon 15 than to *PROSP* (Fig. 3). Therefore, the

Marker	Location, kbp	Allele or repeats	Minor allele frequency	Hetero-zygosity, %	Zygosity in the patient
D3S3681	79894	CA	—	—	heterozygous
D3S1276	85338	CA	—	—	heterozygous
rs9289536	95031	C/T	0.11	0.20	homozygous
rs9713061	95074	G/T	0.10	0.15	homozygous
rs6786905	95213	C/A	0.10	0.18	homozygous
rs13100168	95220	C/T	0.06	0.12	homozygous
rs10433405	95283	G/A	0.14	0.24	homozygous
D3S3556	95525.66	CA	—	—	homozygous
D3S3634	95525.74	CA	—	—	homozygous
D3S1251	95760	CA	—	—	homozygous
D3S3619	97124	CA	—	—	heterozygous
D3S1752	99228	GAT	—	—	heterozygous
D3S3716	100219	CA	—	—	heterozygous
D3S1271	102217	CA	—	—	heterozygous

Minor allele frequencies and heterozygosities of SNPs were calculated from 44 unrelated normal Japanese studied in the International HapMap project. Locations are from NCBI Map Viewer build 36.2. The zygosity analysis was performed for a patient with a deletion in *PROS1*.

Table 1: Description of microsatellite and SNP markers.

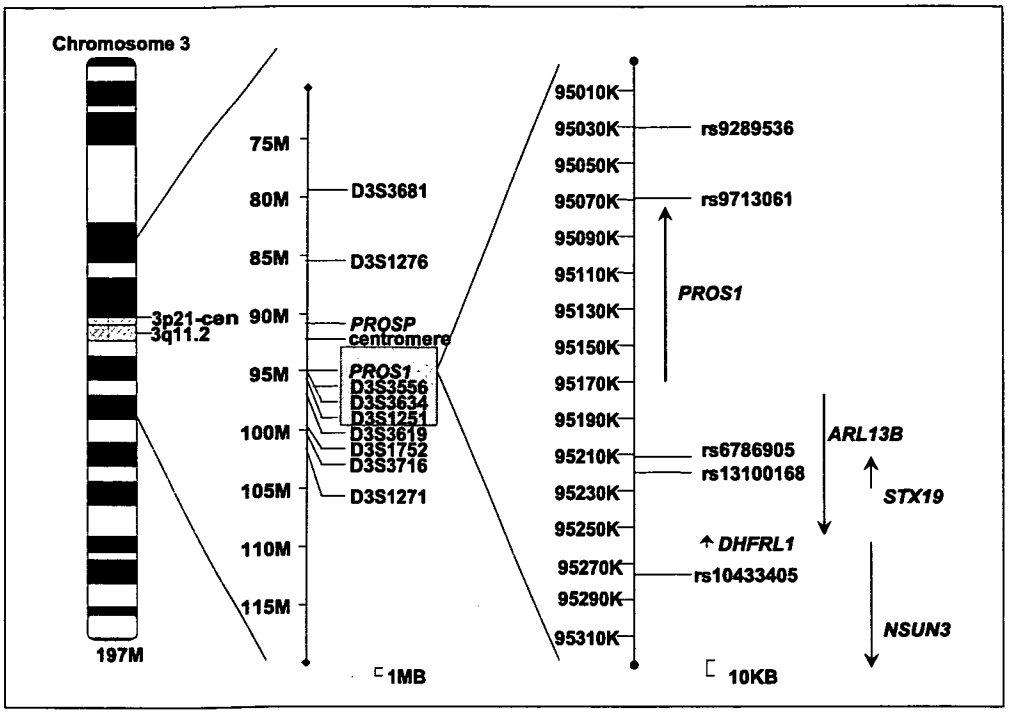

Figure 3: Schematic presentation of the large *PROS1* deletion on chromosome 3. The distributions of *PROS1* (3q11.2), *PROSP* (3p21-cen), *PROS1* flanking SNP and microsatellite markers are mapped on chromosome 3. Possible maximum range of the deletion identified in the patient with DVT is boxed with a grey square. Transcriptional orientations of the genes are shown by arrows. Nucleotide positions are according to NCBI Map Viewer (Build 36.2).

deletion ranged at a maximum from the centromere to before the D3S3619 marker, the first heterozygous marker in the upstream of *PROS1* in chromosome 3. If we take this maximum deletion into account, the large deletion could also include the genes *ARL13B* (ADP-ribosylation factor-like 13B), *STX19* (syntaxin 19), *DHFRL1* (dihydrofolate reductase-like 1), and *NSUN3* (NOL1/NOP2/Sun domain family, member 3), because they are located between *PROS1* and the marker D3S3556 (Fig. 3).

PROS1 deletion carrier in *PROS1* causative point mutation-negative Japanese DVT patients with low PS activity

We measured PC and PS activity in 34 out of 163 DVT patients. We found that 11 patients showed PS activity of less than 50% with PC activity of more than 90%, suggesting functional low PS activity, where the patient with the large *PROS1* deletion was included. Among 11 patients with low PS activity, five carried causative point mutations including missense or splice site mutations (manuscript in preparation by YS and TM). Therefore, in our Japanese DVT patient group, one patient with a large *PROS1* deletion was identified in six DVT patients with low PS activity and no causative point mutations in *PROS1*.

Discussion

With a few exceptions, gene deletion measurements are not routine in most mutation screening studies, and thus alterations of gene deletion on the kilobase scale are thought to be underestimated. By MLPA, Q-PCR, and direct sequencing analysis of the *PROS1* coding regions, in addition to genotyping of the microsatellites and SNP markers flanking *PROS1*, we detected a large deletion encompassing at least the whole *PROS1* coding regions in 1 out of 163 Japanese patients with DVT.

Evaluation of the deletion detection methods

The presence of the highly homologous pseudogene (>96%) *PROSP* hampered the analysis of the gene deletion in *PROS1* by the conventional techniques. In the present study, therefore, we used the MLPA method to detect the deletions in *PROS1*. The accuracy of this method was confirmed by three rounds of MLPA and validated directly by Q-PCR. The presence and possible range of the deletion was further confirmed by direct sequencing of *PROS1* as well as microsatellite analysis and SNP linkage analysis of the flanking regions of *PROS1*. With the sequencing of *PROS1* exon regions, the loss of heterozygosity of all the SNPs of *PROS1* indicates the existence of a hemizygous deletion encompassing the whole *PROS1* gene in one DVT patient. The boundaries of the deletion were deduced by allele zygosity analysis of the SNPs and microsatellite markers centered on *PROS1*. The marker density selected for analysis also has an impact on the accuracy of discriminating the range of the deletion. In the present study, the breakpoints of the deletion could only be limited to the range between D3S3619, which was detected as the first heterozygous microsatellite in the region upstream of *PROS1*, and the centromere located downstream of *PROS1*. To further define the range of the deletion, it will be necessary to determine the segregation pattern of the investigated SNP and microsatellite markers in other affected individuals of the same family (18).

Nature of the large deletion of *PROS1*

The large deletion in the present study was defined as ranging at a minimum distance of 107 kb between the *PROS1* promoter and

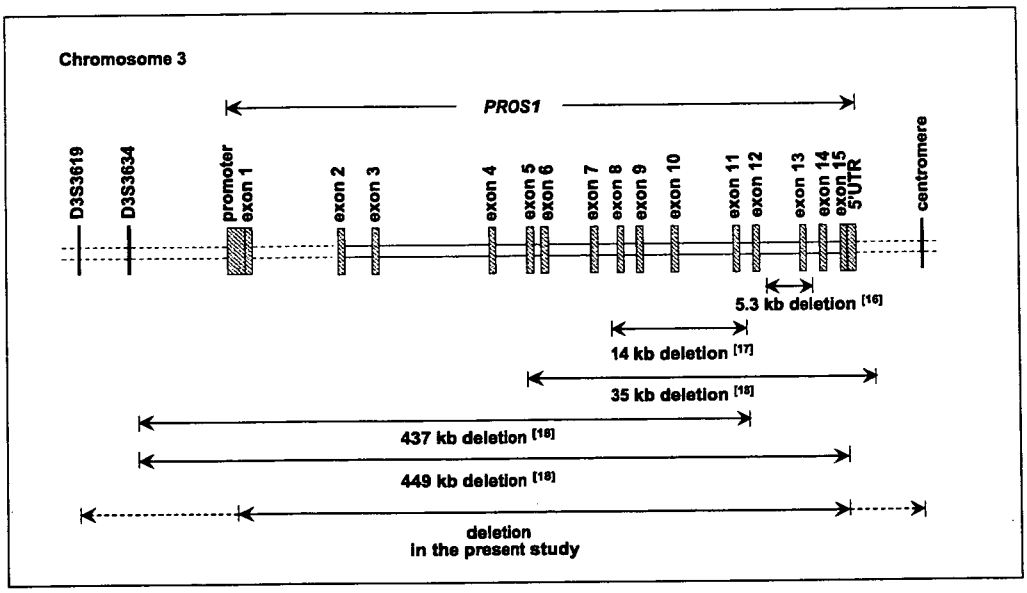

Figure 4: Outline of reported large deletions encompassing *PROS1* on chromosome 3. The location of centromere, *PROS1*, and two upstream microsatellite markers (D3S3619 and D3S3634) are sketched on chromosome 3. The relative long distance between exons 1 and 2 is represented by the dotted line. The distance of the regions flanking *PROS1* is represented by the dotted line. The minimum range of the deletion in the present study is marked with the solid line and the flanking maximum range is marked with the dotted line. The reported deletions are taken from the references (16–18).

exon 15 MLPA probes and at a maximum distance from the centromere to before the D3S3619 marker, the first heterozygous marker in the upstream of *PROS1* in chromosome 3. To date, a total of five large *PROS1* deletions have been described (Fig. 4) (16–18). A 5.3 kb deletion spanning over 90% of intron 12, the entire exon 13, and about a quarter of intron 13, was detected in two *PROS1*-deficient families by Southern hybridization (16). A long-PCR-based technique identified a deletion from intron 7 to 11 that removed approximately 14 kb (17). With a dense set of SNP and microsatellite markers, three large deletions that encompassed at least 35 kb including exons 5–15, 437 kb including exons 1–11, and 449 kb including the whole *PROS1* gene were identified (18). The deletion in the present study was another one with the definite minimum range encompassing the whole *PROS1* gene.

Large deletion of *PROS1* and PS activity

The free PS antigen level and PS activity of the patient with the deletion in *PROS1* were 2.1 μg/ml (normal range: 6.5–9.8 μg/ml) and 16% (normal range: 65–105%), respectively, so that, in addition to the hemi-deletion of the *PROS1* gene, other genetic variations could influence the levels of the PS antigen and activity. However, no causative point mutations were found in this patient by DNA sequencing. If we take the deletion as the maximum, the deletion may encompass four other genes, *ARL13B, STX19, DHFRL1*, and *NSUN3* (Fig. 3). To our knowledge, none of these genes are known to be associated with thrombosis, and thus their absence is unlikely to affect the PS deficiency phenotype. The four genes were also deleted in other patients with PS deficiency (18). Since the characteristics of these genes and the corresponding phenotypes have not yet been clarified, quantitative analysis of these genes was not considered in the present study. Another genetic variation that was missing by our analysis was the existence of chromosomal rearrangements such as an inversion of a large segment of DNA which has been found to be a major genetic defect in the factor VIII gene in patients with severe hemophilia A (30). Mutations in the promoter region might be another possible explanation for the low PS activity. The *PROS1* promoter region has recently been characterized and liver-specific cis-acting DNA elements have been identified, but the role of this region in PS deficiency is still unknown (31).

Mechanism of the large deletion

We speculated that the deletion might occur by non-allelic homologous recombination which can generate rearrangements as a result of recombination between highly similar duplicated sequences, such as segmental duplications (32). It has been confirmed that 24% of the 1,447 copy-number variations in the human genome are associated with segmental duplications. Segmental duplications were more frequently associated with the long copy-number variations (33). However, the segmental duplications were not present in the vicinity of the *PROS1* gene at the pericentromeric region in chromosome 3 (34). Regardless of the recombination mechanism, genomic architectural features have been associated with many rearrangement breakpoints (35). This suggests that the large deletion in *PROS1* is not a random event, but might result from a predisposition to rearrangement due to a complex genomic architecture that may create instability in the genome.

Large *PROS1* deletion in Japanese DVT patients

All of the large deletions of *PROS1* so far reported were detected in affected individuals in PS deficiency families (15–18). In the present study, a *PROS1* deletion was identified in a patient with DVT, but unfortunately, the family members were not available for analysis. The presence of a large deletion in one out of the 163 DVT patients suggested that a large deletion of *PROS1* is relatively rare in DVT patients. However, if the deletion was obtained in specified patients with low PS activity (<50%) and normal PC activity (>90%), it was found in one out of 11 patients. When we looked at DVT patients with low protein S activity who did not carry the causative point mutations in *PROS1*, one out of

six patients had a large *PROS1* deletion. Large deletions in *PROS1* have been previously identified by segregation analysis in three out of eight *PROS1* causative point mutation-negative families with PS deficiency (18). Large deletions of *PROS1* might be more common in familial PS deficiency than previously thought, and MLPA analysis is an effective tool to detect the deletion in *PROS1*.

In conclusion, a large deletion encompassing the whole *PROS1* gene was detected in one DVT patient with 16% PS activity. The large deletion in *PROS1* partly accounted for the low PS activity in patients with DVT. Screening for large deletions in *PROS1* might be warranted in causative point mutation-negative DVT patients with PS deficiency.

Acknowledgements

We would like to thank Dr. Masashi Akiyama and Ms. Junko Ishikawa for their technical assistance.

References

1. Lane DA, Mannucci PM, Bauer KA, et al. Inherited thrombophilia: Part 1. Thromb Haemost 1996; 76: 651–662.
2. Dykes AC, Walker ID, McMahon AD, et al. A study of Protein S antigen levels in 3788 healthy volunteers: influence of age, sex and hormone use, and estimate for prevalence of deficiency state. Br J Haematol 2001; 113: 636–641.
3. Sakata T, Okamoto A, Mannami T, et al. Prevalence of protein S deficiency in the Japanese general population: the Suita Study. J Thromb Haemost 2004; 2: 1012–1013.
4. Beauchamp NJ, Dykes AC, Parikh N, et al. The prevalence of, and molecular defects underlying, inherited protein S deficiency in the general population. Br J Haematol 2004; 125: 647–654.
5. Kimura R, Honda S, Kawasaki T, et al. Protein S-K196E mutation as a genetic risk factor for deep vein thrombosis in Japanese patients. Blood 2006; 107: 1737–1738.
6. Kinoshita S, Iida H, Inoue S, et al. Protein S and protein C gene mutations in Japanese deep vein thrombosis patients. Clin Biochem 2005; 38: 908–915.
7. Miyata T, Kimura R, Kokubo Y, et al. Genetic risk factors for deep vein thrombosis among Japanese: importance of protein S K196E mutation. Int J Hematol 2006; 83: 217–223.
8. Kimura R, Sakata T, Kokubo Y, et al. Plasma protein S activity correlates with protein S genotype but is not sensitive to identify K196E mutant carriers. J Thromb Haemost 2006; 4: 2010–2013.
9. Watkins PC, Eddy R, Fukushima Y, et al. The gene for protein S maps near the centromere of human chromosome 3. Blood 1988; 71: 238–241.
10. Edenbrandt CM, Lundwall A, Wydro R, et al. Molecular analysis of the gene for vitamin K dependent protein S and its pseudogene. Cloning and partial gene organization. Biochemistry 1990; 29: 7861–7868.
11. Ploos van Amstel HK, Reitsma PH, van der Logt CP, et al. Intron-exon organization of the active human protein S gene PS alpha and its pseudogene PS beta: duplication and silencing during primate evolution. Biochemistry 1990; 29: 7853–7861.
12. Schmidel DK, Tatro AV, Phelps LG, et al. Organization of the human protein S genes. Biochemistry 1990; 29: 7845–7852.
13. Gandrille S, Borgel D, Sala N, et al. Protein S deficiency: a database of mutations--summary of the first update. Thromb Haemost 2000; 84: 918.
14. Lanke E, Johansson AM, Hillarp A, et al. Co-segregation of the PROS1 locus and protein S deficiency in families having no detectable mutations in PROS1. J Thromb Haemost 2004; 2: 1918–1923.
15. Ploos van Amstel HK, Huisman MV, Reitsma PH, et al. Partial protein S gene deletion in a family with hereditary thrombophilia. Blood 1989; 73: 479–483.
16. Schmidel DK, Nelson RM, Broxson EH, Jr., et al. A 5.3-kb deletion including exon XIII of the protein S a gene occurs in two protein S-deficient families. Blood 1991; 77: 551–559.
17. Holmes ZR, Bertina RM, Reitsma PH. Characterization of a large chromosomal deletion in the PROS1 gene of a patient with protein S deficiency type I using long PCR. Br J Haematol 1996; 92: 986–991.
18. Johansson AM, Hillarp A, Sall T, et al. Large deletions of the PROS1 gene in a large fraction of mutation-negative patients with protein S deficiency. Thromb Haemost 2005; 94: 951–957.
19. Schouten JP, McElgunn CJ, Waaijer R, et al. Relative quantification of 40 nucleic acid sequences by multiplex ligation-dependent probe amplification. Nucleic Acids Res 2002; 30: e57.
20. Sellner LN, Taylor GR. MLPA and MAPH: new techniques for detection of gene deletions. Hum Mutat 2004; 23: 413–419.
21. Koolen DA, Vissers LE, Pfundt R, et al. A new chromosome 17q21.31 microdeletion syndrome associated with a common inversion polymorphism. Nat Genet 2006; 38: 999–1001.
22. Lai KK, Lo IF, Tong TM, et al. Detecting exon deletions and duplications of the DMD gene using Multiplex Ligation-dependent Probe Amplification (MLPA). Clin Biochem 2006; 39: 367–372.
23. Rooms L, Reyniers E, Wuyts W, et al. Multiplex ligation-dependent probe amplification to detect subtelomeric rearrangements in routine diagnostics. Clin Genet 2006; 69: 58–64.
24. Sakata T, Okamoto A, Mannami T, et al. Protein C and antithrombin deficiency are important risk factors for deep vein thrombosis in Japanese. J Thromb Haemost 2004; 2: 528–530.
25. Hoebeeck J, van der Luijt R, Poppe B, et al. Rapid detection of VHL exon deletions using real-time quantitative PCR. Lab Invest 2005; 85: 24–33.
26. Vandesompele J, De Preter K, Pattyn F, et al. Accurate normalization of real-time quantitative RT-PCR data by geometric averaging of multiple internal control genes. Genome Biol 2002; 3: Research0034.
27. Okuda T, Fujioka Y, Kamide K, et al. Verification of 525 coding SNPs in 179 hypertension candidate genes in the Japanese population: identification of 159 SNPs in 93 genes. J Hum Genet 2002; 47: 387–394.
28. Kimura R, Kokubo Y, Miyashita K, et al. Polymorphisms in vitamin K-dependent γ-carboxylation-related genes influence interindividual variability in plasma protein C and protein S activities in the general population. Int J Hematol 2006; 84: 387–397.
29. Tanaka C, Kamide K, Takiuchi S, et al. An alternative fast and convenient genotyping method for the screening of angiotensin converting enzyme gene polymorphisms. Hypertens Res 2003; 26: 301–306.
30. Lakich D, Kazazian HH, Jr., Antonarakis SE, et al. Inversions disrupting the factor VIII gene are a common cause of severe haemophilia A. Nat Genet 1993; 5: 236–241.
31. Tatewaki H, Tsuda H, Kanaji T, et al. Characterization of the human protein S gene promoter: a possible role of transcription factors Sp1 and HNF3 in liver. Thromb Haemost 2003; 90: 1029–1039.
32. Stankiewicz P, Lupski JR. Genome architecture, rearrangements and genomic disorders. Trends Genet 2002; 18: 74–82.
33. Redon R, Ishikawa S, Fitch KR, et al. Global variation in copy number in the human genome. Nature 2006; 444: 444–454.
34. Bailey JA, Gu Z, Clark RA, et al. Recent segmental duplications in the human genome. Science 2002; 297: 1003–1007.
35. Shaw CJ, Lupski JR. Implications of human genome architecture for rearrangement-based disorders: the genomic basis of disease. Hum Mol Genet 2004; 13: R57–64.

ADAMTS13 assays and ADAMTS13-deficient mice

Toshiyuki Miyata, Koichi Kokame, Fumiaki Banno, Yongchol Shin and Masashi Akiyama

Purpose of review

Thrombotic thrombocytopenic purpura can be induced by acquired or congenital deficiency of the plasma von Willebrand factor-cleaving protease, ADAMTS13. Measurement of ADAMTS13 activity is important for the diagnosis and treatment of microangiopathies including thrombotic thrombocytopenic purpura. Phenotypic analysis of mice lacking the *Adamts13* gene is valuable for understanding the pathogenesis of microangiopathies.

Recent findings

The minimum substrate for ADAMTS13 activity was identified as 73 amino acid residues in the A2 domain of von Willebrand factor, called VWF73. Several new assays have been developed using this sequence. The VWF73-based assays are rapid, quantitative, and easy to handle, and are well correlated with the measures from previous assays. Mice lacking the *Adamts13* gene were produced. The mice were viable and fertile. They showed a prothrombotic state but no symptoms of spontaneous thrombocytopenia, hemolytic anemia, or microvascular thrombosis were observed.

Summary

VWF73-based ADAMTS13 assays will significantly facilitate the accurate diagnosis of microangiopathies and contribute to the improved clinical treatment of these diseases. Accumulated clinical information on patients with ADAMTS13 deficiency and mice lacking the *Adamts13* gene indicates that additional environmental or genetic susceptibility factors are required to trigger thrombotic thrombocytopenic purpura.

Keywords

ADAMTS13, microangiopathy, thrombotic thrombocytopenic purpura, von Willebrand factor

Curr Opin Hematol 14:277–283. © 2007 Lippincott Williams & Wilkins.

National Cardiovascular Center Research Institute, Fujishirodai, Suita, Osaka, Japan

Correspondence to Toshiyuki Miyata, National Cardiovascular Center Research Institute, 5-7-1 Fujishirodai, Suita, Osaka 565-8565, Japan
Tel: +81 6 6833 5012 ext 2512, 8123; fax: +81 6 6835 1176;
e-mail: miyata@ri.ncvc.go.jp

Current Opinion in Hematology 2007, 14:277–283

Abbreviations

CUB	complement components C1r/C1s, Uegf (epidermal growth factor-related sea urchin protein), and bone morphogenetic protein-1
HUS	hemolytic uremic syndrome
TSP-1	thrombospondin type-1
TTP	thrombotic thrombocytopenic purpura
ULVWF	ultralarge von Willebrand factor
VWF	von Willebrand factor

1065-6251

Introduction

Thrombotic thrombocytopenic purpura (TTP) is characterized by thrombocytopenia and microangiopathic hemolytic anemia accompanied by variable-penetrance of neurologic dysfunction, renal failure, and fever. In the microvasculature of patients with TTP, systemic platelet thrombi are developed, largely resulting from the accumulation of ultralarge von Willebrand factor (ULVWF) multimers [1]. ULVWF can be accumulated by acquired or congenital deficiency of the von Willebrand factor (VWF)-cleaving protease, ADAMTS13 (a disintegrin-like and metalloprotease with thrombospondin type 1 motif, 13) [2,3••]. TTP caused by congenital deficiency of ADAMTS13 is also called Upshaw–Schulman syndrome.

Since the cloning of its cDNA in 2001, this new antithrombotic factor has been intensively studied [4–6,7•,8••, 9••,10•]. Here we summarize the recent progress on ADAMTS13, focusing on assays for ADAMTS13 and mice lacking the *Adamts13* gene.

Genetic mutations in congenital ADAMTS13 deficiency

ADAMTS13 consists of 1427 amino acid residues with a calculated molecular mass of 145 kDa. It is composed of multiple discrete domains, as shown in Fig. 1 [4–6,7•,8••, 9••]. Unlike other ADAMTS family members, the ADAMTS13 sequence has a short pro-sequence and two C-terminal CUB [complement components C1r/C1s, Uegf (epidermal growth factor-related sea urchin protein), and bone morphogenetic protein-1] domains. The human ADAMTS13 gene comprises 29 exons, encompassing 37 kb on chromosome 9q34. It is expressed mainly in the liver; primarily in stellate cells [11,12]. Platelets and endothelial cells also express ADAMTS13 [13,14,15•,16••]. The CUB domains are required for apical sorting of ADAMTS13 in endothelial cells [16••].

Figure 1 Genomic structure and domain organization of human ADAMTS13 and nonsynonymous mutations identified in patients with congenital thrombotic thrombocytopenic purpura

Missense mutations are indicated by black spades. Nonsense mutations, insertion/deletion mutations, and splice site mutations are shown by hearts, clubs, and diamonds, respectively. The P475S mutation commonly observed in the Japanese population and the A insertion at nucleotide number 4143 found in multiple European populations are shown. S, signal peptide; P, propeptide; Dis, disintegrin-like domain; T (numbered 1–8), thrombospondin type 1 motifs; CUB, complement components C1r/C1s, Uegf (epidermal growth factor-related sea urchin protein), and bone morphogenetic protein-1; Cys, cysteine-rich domain.

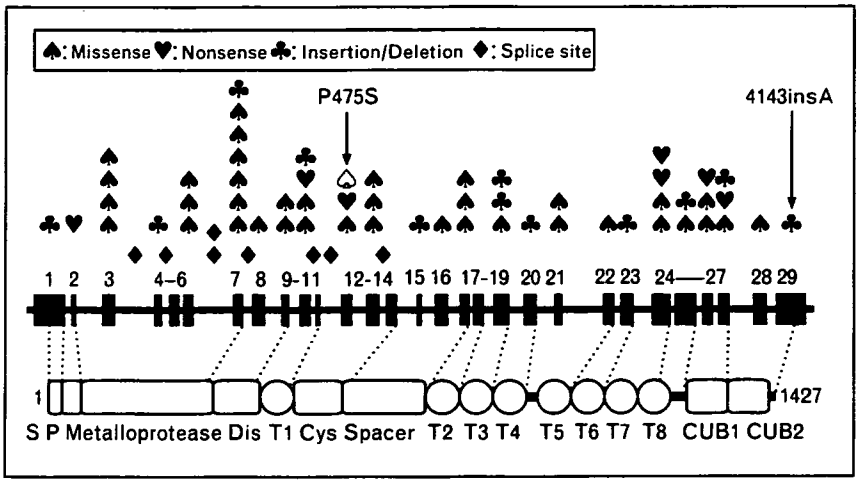

More than 60 different mutations of the *ADAMTS13* gene have been reported [6,17–19,20•,21]. More than 50% are missense mutations, as well as frame-shift mutations such as insertions and deletions, and nonsense mutations and splice-site mutations. These mutations are distributed throughout the various domains of ADAMTS13 (Fig. 1). The correlation of genotype and protease activity in some of these mutations has been examined by expression analysis *in vitro* [18,20•,21]. Most of the mutations have been identified in a single family but there are at least six recurrent mutations in unrelated patients. Among them, the 4143insA mutation has been identified as a genetic background for TTP in multiple families and is frequent among patients with congenital ADAMTS13 deficiency in Northern and Central European countries [22••]. Interestingly, several missense mutations can interact and alter the phenotype of ADAMTS13 deficiency [23••].

There are at least nine missense polymorphisms in the *ADAMTS13* gene. The Q448E mutation was shown not to affect the protease activity, whereas the P475S mutation decreased the activity [18]. This mutation is present in the Asian population but not in the white population [19,24,25]. It has been shown not to be a genetic risk factor for deep-vein thrombosis [26•].

Information regarding the wide variation of phenotypes in TTP patients with congenital ADAMTS13 deficiency has accumulated. Most patients with congenital ADAMTS13 deficiency had their first episode as newborn babies or in early infancy [10•]. After this period, the clinical manifestations of congenital ADAMTS13 deficiency vary from patient to patient, and patients are often incorrectly diagnosed with idiopathic thrombocytopenic purpura or Evans' syndrome during childhood. Seven women with congenital ADAMTS13 deficiency who exhibited TTP at 5–6 months of pregnancy have been reported [27].

The factor V Leiden mutation is a well characterized and the most prevalent genetic risk factor for venous thrombosis. A previous study suggested that the factor V Leiden mutation may be a pathogenic risk factor in patients with thrombotic microangiopathy who have normal ADAMTS13 activity [28]. A recent study did not support the link between the factor V Leiden mutation and thrombotic microangiopathy [29].

Hemolytic uremic syndrome (HUS) is a thrombotic microangiopathy with manifestations of hemolytic anemia, thrombocytopenia, and renal impairment [1,8••,9••,30]. In most cases, typical HUS is triggered by Shiga toxin-producing *Escherichia coli* and manifests diarrhea (D+HUS). Atypical non-Shiga toxin-associated HUS is not associated with diarrhea (D−HUS), and deficiencies of complement factor H, membrane cofactor protein, and complement factor I have been reported in such atypical HUS [9••,31].

Epitopes of ADAMTS13 autoantibodies

Inhibitory autoantibodies for ADAMTS13 cause a deficiency of ADAMTS13 among patients with autoimmune TTP [3••,8••]. The prevalence of ADAMTS13 deficiency among patients with TTP varies from 13 to 100% depending on the criteria of the study. TTP may develop within 2–6 weeks after the antiplatelet agent ticlopidine is administered. TTP may develop in patients with HIV infection. No other apparent etiologies of inhibitory autoantibodies have been identified.

Several studies using recombinant ADAMTS13 and its truncated forms have identified the epitopes of

autoantibodies in patients with TTP. Many inhibitory autoantibodies recognized the spacer domain as the target epitope [32–34,35•]. Some reacted with the C-terminal CUB domains and the first thrombospondin type-1 (TSP-1) repeat [33]. Multiple B-cell clones producing antibodies directed against the spacer domain have been reported [36].

Assays of ADAMTS13 activity

ADAMTS13 assays such as multimer analysis by SDS/agarose-gel electrophoresis and residual collagen-binding analysis have been utilized for plasma ADAMTS13 activity in thrombotic microangiopathies and other pathophysiological conditions [2,4,6]. These assays quantify ADAMTS13 activity by measuring residual VWF multimers or their activity, suggesting that more accurate and simpler assays are in demand.

New assays using VWF73 peptide as the ADAMTS13 substrate

In 2004, we identified a 73-amino acid sequence spanning residues D1596–R1668 of the VWF A2 domain, VWF73, as the minimum region for ADAMTS13 cleavage [37]. A shorter peptide, VWF64, from D1596 to R1659, was not a good substrate for ADAMTS13. Since the development of VWF73 as the substrate for ADAMTS13, several new assays based on the VWF73 sequence have been developed [37–39,40•–43•]. So far, seven assays have been published for the VWF73-based measurements of ADAMTS13 activity. The characteristics of these assays are summarized in Table 1 [37–39,40•–43•]. The assays have the advantages of being simple, rapid, accurate, and quantitative. They do not require denaturing conditions; therefore, the incubation time of the substrates and plasma samples is reduced to less than 1 h. They give rise to quantitative measures. In addition, most of the assays are compatible with the 96-well microplates that clinical-laboratory workers are familiar with, so they have the potential to be widely used in clinical settings.

Of the seven assays, FRETS-VWF73, a fluorogenic substrate for ADAMTS13, is well characterized. The advantage of using FRETS-VWF73 is that the ADAMTS13 activity can be determined by the initial velocity of the increase in fluorescence. Therefore, the assay is highly quantitative. ADAMTS13 cleaves VWF with a $K_m$app of 3.7 ± 1.4 μg/ml or 15 nM in VWF subunits, which is comparable with the plasma VWF concentration of 5–10 μg/ml, and with a value for k_{cat} of ~0.83 min^{-1} [44•]. ADAMTS13 cleaves FRETS-VWF73 with a $K_m$app of 3.2 ± 1.1 μM and a k_{cat} of ~58 min^{-1}. Thus, the affinity of ADAMTS13 to FRETS-VWF73 was decreased ~200-fold compared with VWF, but the catalytic efficiency was ~70-fold greater than VWF. Therefore, ADAMTS13 cleaves VWF and FRETS-VWF73 with roughly comparable catalytic efficiencies of 55 and 18 μM^{-1} min^{-1}, respectively [44•].

FRETS-VWF73 was evaluated by three different research groups [45–47]. Although the definitive evaluation remains to be determined in a large cohort of patients diagnosed with acquired or congenital TTP, ADAMTS13 activity determined by FRETS-VWF73 assay was in good accordance with that measured by conventional assays. FRETS-VWF73 is now commercially available (Table 2).

There may be limitations of the VWF73-based ADAMTS13 assays. VWF73, a small fragment of the A2 domain of VWF, may lack additional sites on VWF that interact with ADAMTS13. The A1 domain of VWF binds cofactors such as platelet glycoprotein Ib and heparin to regulate cleavage [48], and the A3 domain may be a docking site for ADAMTS13 [49]. VWF73 lacks

Table 1 VWF73-based ADAMTS13 activity assays

Substrate	Principle	Reference
GST–VWF73 fusion protein with the C-terminal 6×His tag	Western-blot detection using anti-GST antibody	[37]
FRETS-VWF73, synthetic VWF73 peptide with a fluorophore at the P7 position and a quencher at the P5′ position	Fluorescence resonance energy transfer, initial-velocity method	[39]
Immobilized GST–VWF73 fusion protein with the C-terminal 6×His tag	Enzyme immunoassay, the amount of 6×His remaining was assayed with anti-6×His IgG conjugated with HRP, end point method	[38]
Immobilized His- and biotin-labeled VWF73 conjugated with HRP	Enzyme-linked assay, endpoint method	[40•]
Immobilized GST–VWF73 fusion protein with the C-terminal 6×His tag	Mass-spectrometry analysis of the products, endpoint method	[41•]
Immobilized GST–VWF73 fusion protein with the C-terminal 6×His tag	Enzyme immunoassay, the amount of products were assayed with anti-N10 mAbs conjugated with HRP, endpoint method	[42•]
Recombinant 6×His-tagged VWF73 peptide labeled with fluorescein at both the P7 and P6′ positions	Fluorescence resonance energy transfer, initial-velocity method	[43•]

GST, glutathione-S-transferase; HRP, horseradish peroxidase; mAb, monoclonal antibody; VWF73, 73 amino acid residues of von Willebrand factor (VWF) from D1596 to R1668.

Table 2 Commercially available kits for assaying ADAMTS13 activity and antigen

Kit	Maker/supplier	Objectives	Time
FRETS-VWF73	Peptide Institute, Peptides International	Activity	1 h
ATS-13 ADAMTS-13 Activity	GTI	Activity	30 min
ADAMTS13 ELISA kit	Mitsubishi Kagaku Iatron	Antigen	3.5 h
ADAMTS13 activity ELISA kit	KAINOS LABORATORIES	Activity	3.5 h
TECHNOZYM ADAMTS-13	Technoclone GmbH	Activity/antigen	2.5 h/4 h
TECHNOZYM ADAMTS-13 INH	Technoclone GmbH	Autoantibody	2.5 h
ACTIFLUOR ADAMTS13 Activity Assay kit	American Diagnostica	Activity	
IMUBIND ADAMTS13 ELISA	American Diagnostica	Antigen	5 h
IMUBIND ADAMTS13/fXI Complex ELISA	American Diagnostica	ADAMTS13/FXI complex	4 h
IMUBIND ADAMTS13 Autoantibody ELISA	American Diagnostica	Autoantibody	4 h

these domains. Therefore, if enzyme defects in patients with TTP affect the ADAMTS13-binding site for these domains, cleavage of VWF73 will not reflect these defects.

Measurements of ADAMTS13 autoantibodies

Autoantibodies neutralizing ADAMTS13 activity are a major cause of acquired TTP. The presence or absence of inhibitory autoantibodies is important in discriminating acquired from congenital TTP. An inhibitor assay is generally carried out using mixtures of heat-inactivated plasma from patients and normal plasma at a 1:1 dilution or several dilutions. Assays for ADAMTS13 activity so far developed, including VWF73-based assays, are compatible for the inhibitor assay. It should be noted that nonneutralizing autoantibodies may reduce the circulating ADAMTS13 levels by antibody-mediated clearance.

ELISA has been developed to detect autoantibodies against ADAMTS13. In this process, immobilized ADAMTS13 in the plate wells captures both inhibitory and noninhibitory autoantibodies in plasma samples; then secondary detection antibodies, such as goat antihuman IgG or IgM antibodies labeled with horseradish peroxidase, are added and the levels of ADAMTS13-binding IgGs are determined [50]. Using this assay, low titers of IgG antibodies were detected in four out of 111 healthy control donors who lacked anti-ADAMTS13 inhibitory activity by inhibitor assays. IgG autoantibodies were found in 97% of untreated patients with acute acquired thrombotic microangiopathies who had plasma ADAMTS13 activity levels below 10% [51]. This assay was more sensitive than the standard functional inhibitor assay for detecting autoantibodies against ADAMTS13. The ELISA kit utilizing this principle is now commercially available (Table 2), and has been validated to be useful [52].

Antigen assays for plasma ADAMTS13

ELISA for measuring plasma ADAMTS13 antigen levels has also been developed by several research groups. ADAMTS13 antigen ELISA kits are also commercially available (Table 2).

Healthy plasma ADAMTS13 levels

The ELISA assay to detect plasma ADAMTS13 levels can estimate the plasma ADAMTS13 concentration when the ADAMTS13 standard can be obtained from recombinant full-length ADAMTS13 protein. The ADAMTS13 antigen concentration in normal human plasma pooled from white donors was 1.03 ± 0.15 μg/ml of plasma [53•]. Interestingly, normal Chinese donors have significantly lower antigen levels (0.62 ± 0.13 μg/ml). In another study of 99 healthy Austrian donors, the median plasma ADAMTS13 level was 1.08 μg/ml using recombinant ADAMTS13 as the standard [54•]. The plasma ADAMTS13 level in Japanese donors was reported to be 0.82 ± 0.15 and 0.70 ± 0.13 μg/ml using two different ELISA systems when recombinant ADAMTS13 was used as the standard [55•].

Phenotype of mice lacking *Adamts13* gene

The mouse is a promising animal model for seeking genetic or environmental susceptibility factor(s) for a certain disease phenotype. Two types of mouse *Adamts13* cDNA have been isolated and characterized [56]. cDNA isolated from the 129/Sv strain showed a domain organization identical to the human one. The other cDNA lacked the C-terminal two TSP-1 motifs and two CUB domains due to the insertion of an intracisternal A particle retrotransposon in intron 23, which creates a premature stop codon. Both recombinant proteins showed VWF-cleaving activity *in vitro*.

Mice lacking the *Adamts13* gene have been recently developed by us and another group [57,58••,59••]. We generated mice lacking the *Adamts13* gene by replacing exons 3–6 encoding the catalytic domain by a neomycin-resistant cassette and analyzed phenotypes on a 129/Sv genetic background of the ADAMTS13-deficient mice [58••]. The ADAMTS13-deficient mice were born in the expected Mendelian distribution. Plasma from homozygous mice showed no ADAMTS13 activity. The mice were viable and fertile. Hematologic and histologic examinations failed to detect any evidence of thrombocytopenia, hemolytic anemia, or microvascular thrombosis. However, ULVWF multimers were observed in the plasma of homozygotes. Thrombus formation on immobilized